Master's Thesis

Adaptive Automatic Transmit Power Control

Michail Triantafyllidis

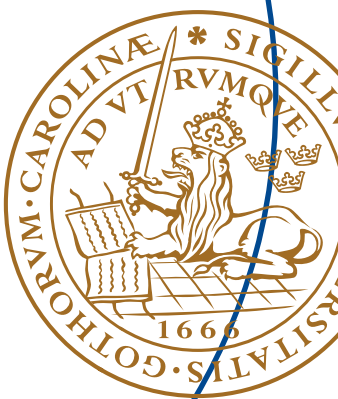

Department of Electrical and Information Technology,
Faculty of Engineering, LTH, Lund University, June 2014
In cooperation with Ericsson AB.

Master's Thesis

Adaptive Automatic Transmit Power Control

By

Michail Triantafyllidis

Supervisors
Sima Shahsavari, Ericsson
Fredrik Tufvesson, Lund University

Department of Electrical and Information Technology
Faculty of Engineering, LTH, Lund University
Lund, Sweden

Abstract

In addition to the sharp growth of mobile broadband users, the use of modern network access technologies increases significantly the traffic into the backhaul networks. The capacity of the Mobile Backhaul Networks (MBNs) is limited and upper bounded by the available spectrum, which is an expensive and finite natural resource. Nowadays, it is critical to enable tighter frequency reuse in MBNs in order to increase the spectral efficiency and to lower the costs in specific markets.

The main propagation phenomena that deteriorate the communication of microwave links are the flat fading and the frequency selective fading. In order to compensate for the fading, the automatic transmitter power control (ATPC) and linear equalization are used. Using the ATPC could increase the interference in MBN. Furthermore, the tighter frequency reuse introduces additional interference in MBNs which can result in performance degradations as well as additional outages.

Power control and interference cancellation are two potential techniques to enable a tighter frequency reuse in MBNs. In [1], a clever power control technique, called Node ATPC, is suggested to maintain the Signal-to-Interference-plus-Noise Ratio (SINR) of unfaded links as well as to compensate for the rain fading at the faded links. Nevertheless, the technique suffers from lack of optimality, network utilization and power efficiency due to the fact that the interference imposed by applying ATPC to one link would not necessarily affect all other links of MBN in a similar way. Furthermore, the knowledge of MBN channel matrix permits the design of an optimal power control algorithm by considering the interaction between each link pair of MBN network.

This thesis investigates and evaluates an optimization strategy for the proposed adaptive node ATPC. The suggested power control algorithm is called optimized-ATPC and it is using a novel mathematical formulation [2] that maximizes the network utilization and minimizes the power consumption using the convex optimization technique.

The introduced power control algorithm is evaluated and compared with the node APTC algorithm with respect to the frequency reuse, spectral efficiency and power consumption using different network topologies and antenna types. The results clarify that the proposed power control technique can be used to achieve tighter frequency reuse and better network performance.

Acknowledgments

This section of my thesis is dedicated to the people that helped me during my Master thesis and they were next to me and supported me during my studying period in Lund University.

Foremost, I would like to express my sincere gratitude to my supervisor in Ericsson, Sima Shahsavari, for giving me the opportunity to work in the biggest worldwide telecommunication company, Ericsson AB. Working with Sima Shahsavari was a great experience; she helped me in all the time of research and writing of this thesis and I feel grateful for her continuous support, patience, motivation, enthusiasm, and immense knowledge.

My sincere thanks also go to my supervisor in Lund University, Fredrik Tufvesson. Except from guiding me during this thesis, he offered me summer internship opportunity in his group. During the summer internship I had the opportunity to work with the experienced researcher Ghassan Dahman.

Besides my supervisors, I would like to thank the rest of the people, who were next to me during my studies in Lund University. My family, my friends and all the people, who made my studying experience in Lund University a very special part of my life.

Michail Triantafyllidis

Table of Contents

CHAPTER 1

1 Introduction

This report will present the theory, the methodology and the results of the Master of Science thesis performed at Ericsson AB during the academic year 2013-2014.

This chapter gives a general description of the frequency reuse concept and the power control problem. Finally, the goal of the thesis is set.

1.1 Introduction and Background

The Mobile Backhaul Network (MBN) unites a mobile access network with transport/packet networks [3]. The deployment and the design of MBNs potentially affect the overall network operation and performance. MBNs are expanding rapidly and are covering wide areas of the globe. The reason that the operators prefer to install MBN instead of other types of backhaul networks is their low installation cost, high performance and deployment flexibility.

Nowadays, MBNs must be designed in order to achieve high data rates, provide different types of wideband services and support the data traffic that is generated by the evolutionary radio access networks (e.g. LTE, WCDMA). In detail, the traffic that must be handled by the links of MBN is increasing rapidly and the proper operation of the inter-element connections should be ensured.

MBNs are consisted of a large number of connections between base stations which are called microwave links. The physical layer technology of MBN is not strictly defined and is adaptive to the propagation conditions (adaptive modulation and coding).

According to [4], it is estimated that the mobile-broadband traffic is increasing dramatically. In Figure 1.1, the estimation of the global mobile traffic raise [5] is depicted. As a result of the traffic growth, the operator's capacity bottleneck will be MBN due to its relatively narrow frequency

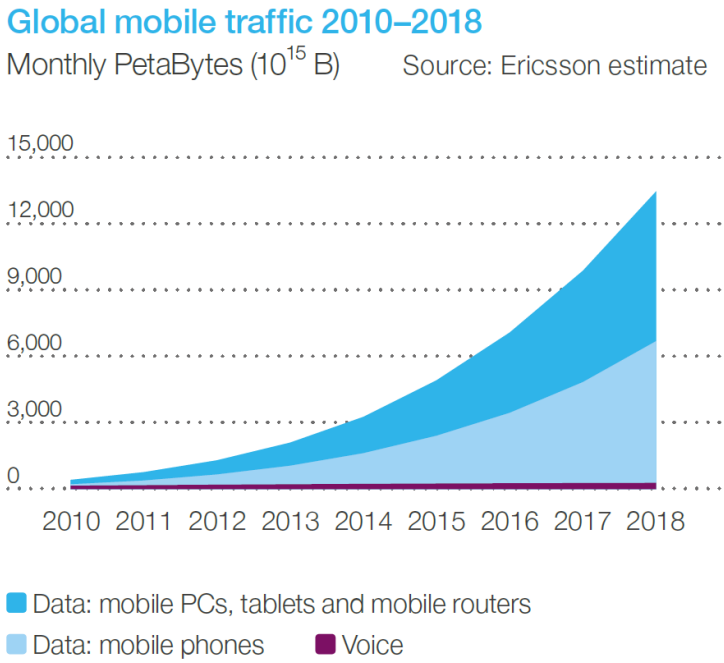

Figure 1.1: Estimation of the Global Mobile Traffic 2010-2018 by Ericsson [5]

channel and lack of spectrum [6]. The need for tighter frequency reuse and better spectrum efficiency is becoming critical.

A microwave radio link is a full duplex wireless communication system. In order to establish communication in both directions, microwave links are usually deployed using Frequency Division Duplex (FDD) technique. In FDD systems, the frequencies that are allocated for the uplink and the downlink are different and have a constant and predefined duplex space.

The licensing process for the installation of the microwave links is quite complex as the operator has to apply for a license for each microwave link separately. Furthermore, the license is customized to one microwave link with specific assigned frequency, output power level and antenna mask. The license details depend on the interference to and from the other microwave links.

The construction of an MBN is unique and depends on the required network capacity, the number of operators on the market, local regulations, terrain, propagation conditions, cost limit etc. Given an MBN infrastructure and an available frequency spectrum, an operator can achieve better capacity by applying a tighter frequency deployment strategy. Especially in

some markets that the available spectrum allocated for microwave radio links is very limited, the need for tighter frequency usage is essential.

1.2 Purpose

The goal of this thesis is to investigate and evaluate innovative power control techniques that enable a tighter frequency reuse in MBNs.

In many traditional microwave links, to overcome a possible fading due to rain, the power of a transmitter is usually fixed to a higher power level including the fade margin. This results in an unnecessary strong signal power during clear sky conditions, which imposes increased interference to the other microwave links of MBN. Instead of always using a fixed transmit power, one could adjust the transmitters power dynamically during fading. Thus, utilize a lower transmit power during clear sky conditions. This power control technique referred to as Automatic Transmit Power Control (ATPC).

In [1], a study about the effect of power control and interference cancellation techniques on the frequency reuse in MBN is carried out. As it is shown in [1], the limiting factor of frequency reuse is the rain fading as in this case more frequencies must be used to ensure that MBN will be operational.

In dense environments it is common to use star topologies, with many links joined to a common node. The use of ATPC in one hop, however, could expose un-faded, outer radios for an excessive amount of interference. In [1] this issue is suggested to be overcome by coordinating ATPC within the center node to let unfaded links increase their output powers accordingly to compensate for the excessive interference. This technique is called node ATPC [1]. Node ATPC is a clever technique to maintain the Signal-to-Interference-plus-Noise Ratio (SINR) of the unfaded links as well as to compensate for the rain fading at the faded links. Thus, possibly prevent an outage. Nevertheless, the technique suffers from lack of optimality, low spectrum efficiency and low power efficiency. This is due to the fact that the interference imposed by applying ATPC to one link would not affect all other links in the same way. There might be some links with no impact and no need for any compensation in their output power. One may also realize that all other affected links do not suffer from the same level of interference. An adaptive power control technique could be a solution to adjust the output power of the microwave links in more optimal way by considering the interaction between each pair of them.

This thesis introduces a new optimized power control algorithm for that utilizes the entire network topology information for the power allocation strategy. The suggested power control technique employees a novel mathematical formulation [2] that maximizes the network utilization and minimizes the power consumption using the convex optimization technique.

1.3 Problem Formulation

Will the usage of the power control optimization technique [2] improve the frequency reuse and the spectral efficiency of the Mobile Backhaul Network?

1.4 Related Work and Thesis Contributions

This master thesis intends to study if the application of a novel mathematical formulation of the power control problem [2], which uses convex optimization, can enable tighter frequency reuse, improve the spectral efficiency and decrease the power consumption in an MBN.

In [7], it is shown that the ATPC technique can be used to improve the spectral efficiency of microwave links by adjusting the transmit power to a level that ensures a constant bit error rate (BER), regardless of the propagation conditions. This technique is called hop-ATPC as it is applied on a link basis. Applying hop-ATPC, the total interference in MBN is reduced as the used transmit power during clear sky conditions is lower. This enables tighter frequency reuse and provides a spectral efficiency gain. The investigations made by [7] emphasizes that implementing ATPC in the 38 GHz band not only provides significant improvement in the spectral efficiency (from ~50% to ~70%), but also reduces the maximum bandwidth consumption (from ~300 MHz to ~180 MHz).

In [1], the node cancellation and the node ATPC techniques in an MBN are introduced and are evaluated when these methods are applied to different network topologies. While in hop-ATPC the power of each link is regulated independently, in node ATPC the decisions for the power level of the microwave links are taken in a center node that the microwave links are connected.

The node cancellation technique utilizes the technology that is used at the Cross-Polarization Interference Cancellation (XPIC) [8] to reduce the

interference level. The node cancellation is meant to reduce the co-channel interference of the microwave links that are connected to the same node while the XPIC is used to reduce the cross-polar interference while.

Within a wide range of the existing literature on the power control optimization, the work presented in [2] can be applied for power control of MBNs. The presented algorithm is used to optimize the power allocation for a single-channel network under predefined QoS constraints assuming that the channel information is available.

The master thesis provides an insight on how the optimized power control (optimized-ATPC) algorithm could be applied and combined with frequency deployment algorithms in order to enable a tighter frequency reuse in an MBN.

1.5 Report Outline

In Chapter 2, a brief introduction into the relevant theory behind the Mobile Backhaul Network architecture is provided.

In Chapter 3, the power control technique using the convex optimization technique is analyzed.

In Chapter 4, the system setup, the case study and the frequency deployment algorithms are explained and analyzed. Moreover, the antenna models, the assumptions and the parameters used in the implementation of the simulator are described and motivated.

In Chapter 5, the power control algorithms hop-ATPC, node-ATPC and optimized-ATPC are compared in terms of frequency reuse and spectral efficiency. The superiority of optimized-ATPC over hop-ATPC and node-ATPC is demonstrated using different propagation scenarios and network topologies.

CHAPTER 2

2 Theoretical Background

This chapter is a brief introduction into the relevant theory behind the Mobile Backhaul Network architecture, which is found essential to understand this thesis work.

2.1 Mobile Backhaul Network Architecture

The mobile backhaul network connects the Radio Base Station (RBS) site and the switch site at the edge of a transport network [9]. MBN is divided into two distinct parts (Figure 2.1):

a) The Low Radio Access Network (LRAN)
b) The High Radio Access Network (HRAN)

The LRAN is usually microwave based. It aggregates traffic from several RBS (10 to 100 RBS) and feeds it into the HRAN. The HRAN typically aggregates the traffic from several LRANs using an existing fiber or microwave network, such as the metro network. The physical layer of the LRANs varies and depends on the operator's strategy and availability at the site.

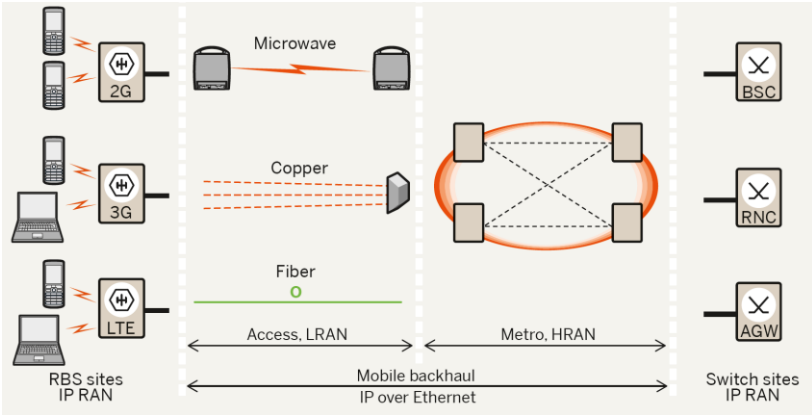

Figure 2.1: Mobile Backhaul Architecture [9]

The LRAN must be simple, cost-effective, upgradable and flexible. Nowadays, the microwave is the dominating backhaul technology because of its low cost deployment and high capacity. It should be mentioned that both fiber and copper consist a common backhaul solution in many parts of the world [9].

A sharply rising demand for mobile data services was caused by the successful launch of mobile broadband services, which are based on high-speed packet access (HSPA) radio networks. This trend is continuing with the rollout of HSPA Evolution and Long Term Evolution (LTE), which will increase the need for high backhaul capacity [9].

The fiber access is commonly used for high-speed links as the capacity that it offers exceeds any LTE backhaul requirement so far [10]. Today, the microwave's and copper's physical layer technologies permit for reaching the level of Gbps capacity.

In order to meet the capacity requirements for LTE and HSPA, the backhaul capacity must be increased by using new frequencies or by increasing the spectral efficiency.

The utilization of vertical and horizontal polarization of the electromagnetic waves can be used in a smart way to double the capacity of microwave links: two different carriers on the same frequency channel can be transmitted using horizontal and vertical polarization. What is more, the XPIC technique [8] can be used to suppress the interference between the polarizations.

Another way to increase the spectral efficiency is to use higher order modulation schemes and achieve higher rates using the same bandwidth. However, the higher order modulation schemes need higher SINR, which

can be achieved by using larger antennas with higher gains. Thus, an extra manufacturing cost is applied for the operator.

Finally, modern multiplexing methods (e.g. orthogonal frequency division multiplexing - OFDM) and multiple antenna techniques (MIMO) can be used to increase the data rates and the spectral efficiency.

By permitting multiple routes to and from the RBS, the capacity and the stability of MBN are increasing significantly. As far as MBNs topology are concerned, the chain topology has been replaced by the star shaped topology, where multiple microwave links end up to one RBS. The different kinds of network topologies that are applied in microwave based MBNs are described in detail in the section (2.4.1).

2.2 Frequency Planning

2.2.1 Frequency Planning Objectives

The goal of the frequency planning is to assign the minimum number of frequencies to MBN's microwave links with respect to the required link quality and level of interference in the network [11].

During the frequency planning process many aspects are taken into consideration. Thinking over the propagation conditions (path length, site location, terrain topography, and atmospheric effects), a frequency band that is suitable for the specific case is determined. Within the appropriate frequency band, the frequency subset that minimizes the mutual interference (e.g. interference among radio frequency channels in the actual path, interference to and from other radio paths, interference to and from satellite communication systems) must be selected. Furthermore, the selected bandwidth must be enough in order to support the required capacity.

2.2.2 Frequency Channel Arrangements

The available frequencies are grouped into segments that are called channels. Depending on the required capacity of the link, every channel has a specific bandwidth, which defines the maximum number of carriers that can be supported [11].

FDD technique is used to support full-duplex communication in microwave links. The available frequency band is divided into two equal halves for transmitting and receiving purpose (Figure 2.2).

The duplex spacing is defined by the difference of the lowest frequency in the lower half and that of the upper half. The duplex spacing must be sufficiently large in order to have interference-free duplex communication.

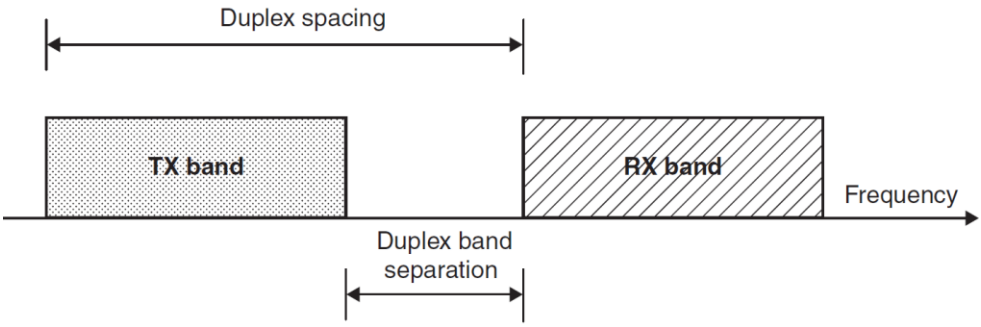

Figure 2.2: Frequency band and FDD [11]

2.2.3 Frequency Regulations and Standards

The International Communication Union (ITU), and specifically the Radiocommunications Sector (ITU-R), is responsible for the frequency administration of a frequency band for the purpose of its use by one or more services [11].

ITU guarantees the efficient use of the radio spectrum, without introducing excessive interference, and determines the international recommendations regarding the radio planning and the operational procedures [12]. The ITU spectrum plan divides the world into three regions, as it is shown in Figure 2.3: America, Europe/Africa and Asia/Pacific.

The frequency allotment is usually done by one administration in one or more countries or geographic regions [11]. The regional plans are defined mainly by the Conference of European Post and Telecommunications administrations (CEPT) and the Federal Communications Commissions (FCC) of the United States of America [12].

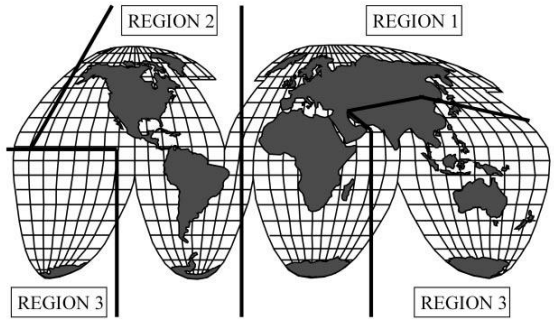

Figure 2.3: ITU-R regions [12]

2.3 Microwave Radio

In this subsection, the basic characteristics of a microwave link are described.

2.3.1 Maximum Transmitter Power and Power Control

The maximum transmitter power is one of the fundamental components that define the overall system range. The signal strength potentially affects the capability of the receiver to decode the signal correctly, even during periods of heavy interference or radio fading (e.g. bad weather conditions).

Depending on the microwave's operation frequency, the typical specified transmitter power level varies from 15 dBm to 25 dBm [12]. The connection of the power level between dBm and $Watts$ is given by the following formulas:

$$P[dBm] = 10\ log_{10}\left(\frac{P[W]}{10^3}\right) \tag{2.1}$$

$$P[W] = 10^{((P[dBm]-30)/10)} \tag{2.2}$$

While a high transmission power can result in increased signal power at receiver's side, the use of fixed high transmission power can lead to a dramatic increase in the interference levels during clear sky conditions. A simple version of the problem is demonstrated in Figures 2.4 and 2.5. In Figure 2.4, a microwave transmission during heavy rain is depicted. Both the SINR at A and B will be enough for the links to be operational. In this

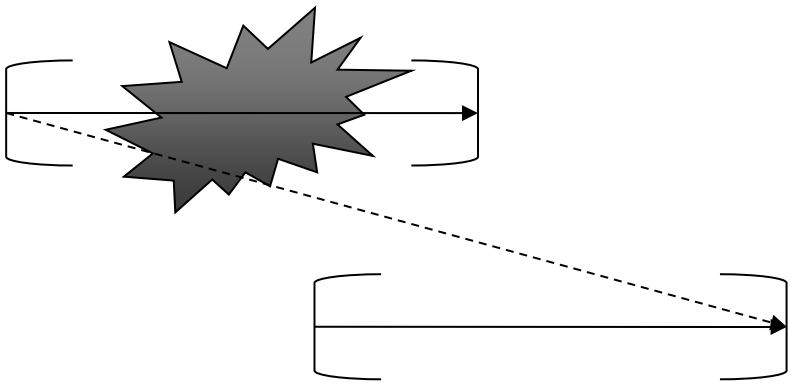

Figure 2.4: Microwave transmission during bad weather conditions. Faded signal and interference

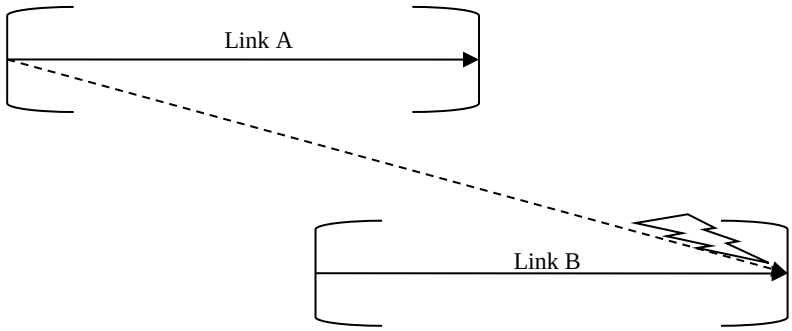

Figure 2.5: Microwave transmission during clear sky conditions. High level of interference at Link B.

case, if the maximum transmission power is used, the signal strength at link A will increase and the SINR at link B will not be decreased. In Figure 2.5, a microwave transmission during clear sky conditions is illustrated. Using the maximum transmission power at link A, the level of interference at link B will be high and probably the SINR of the link B is not sufficient for the normal operation of the link.

In order to compensate for the fading during bad weather conditions and handle the minimum level of interference during clear sky conditions, many radio system manufacturers offer a feature called ATPC. Using this feature,

the minimum power that is needed for each microwave transmission is utilized.

2.3.2 Receiver Sensitivity

The receiver's sensitivity threshold is defined as the minimum received signal power required by the receiver in order to decode the signal accurately. The level of accuracy is measured by the maximum achievable BER. The level of receiver sensitivity depends on the target BER, the data rate, the operation frequency and the modulation scheme.

2.3.3 Noise Power

Noise power is the total degradation of the Signal-to-Noise-Ratio (SNR) of the system due to the thermal noise and the noise factor of the circuit [13]. Thermal noise is generated as a result of thermal agitation of the electrons within an electrical conductor [13]. The thermal noise power at the receiver is given by:

$$P_n = k_b T B \tag{2.3}$$

where $k_b = 1.379 \times 10^{-23} \left[\frac{W}{Hz\,K}\right]$ (Boltzmann's constant), $T\,[K]$ is the absolute temperature of the input noise source and $B\,[Hz]$ is the effective noise bandwidth of the system [13]. The noise power is given by:

$$N_{out} = P_n F \tag{2.4}$$

where F is the noise Figure of the receiver.

2.3.4 Receiver Overload

The receiver overload can happen if the receiver signal exceeds a maximum permitted power level. This in turn results in unacceptable reception quality and may destroy the receiver [13]. The limit of the allowable signal strength at the receiver is given for a specific BER level.

2.3.5 Frequency Stability

The frequency stability expresses the deviation of the actual center frequency from the defined center frequency of the chosen radio channel [13]. Employing Phase Locked Loop (PLL) circuitry, a typical frequency stability of $\pm 0.0015\%$ is expected.

2.3.6 Sensitivity to Interference

Adjacent channel interference is caused by the operation of microwave links in adjacent radio channels [13]. The receiver must compensate for this interference level and maintain the BER under a specified level. Typical Carrier to Interference (CIR) levels for adjacent interference are -10 to $-12\ dB$ for BER 10^{-6}. This means the interfering signal can be 10 to $12\ dB$ higher than the carrier signal.

Co-channel interference is caused by the microwave links that use the same frequency channel [13]. A typical CIR level that a microwave link can handle is $+13\ dB$ for BER 10^{-6}. In this case the carrier signal must be $13\ dB$ stronger than the interfering signal.

2.3.7 Radio Tuning Range

The radio tuning range defines the spectrum width within which the microwave link should operate. The wider the tuning range of a radio, the more channels it can use.

2.4 Network Design

2.4.1 Network Topologies

Several different network topologies can be used for MBNs. The performance, the cost, and the reliability will be strictly affected by the selected topology. The most commonly used topologies are described below.

2.4.1.1 Chain Topology

Chain network topology consists of links in a chain such that every base station (BS) in the chain acts as an active repeater for the previous one [11]. This type of network topology permits tight frequency reuse. However, the overall performance of the network is depending on the propagation characteristics of any individual hop. Furthermore, a link failure can cause serious downtimes as no alternative route is available. In order to increase the reliability of this network structure usually additional links are added across the network to provide some kind of redundancy. In such a topology base stations that are located closer to the Base Station Controller (BSC) will have higher capacity. The chain topology is illustrated in Figure 2.6.

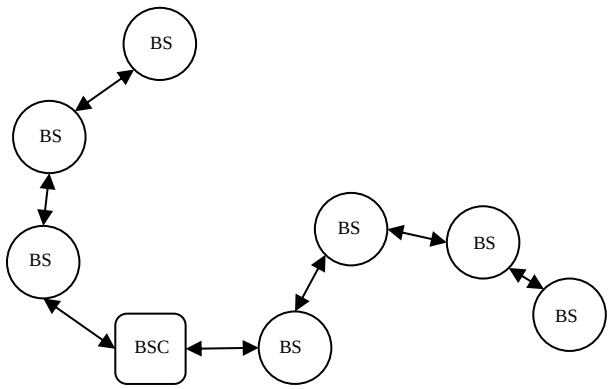

Figure 2.6: Chain Topology

2.4.1.2 Simple Star Topology

In Figure 2.7 the simple star topology [11] is represented. As can be found from the Figure, all the base stations are connected directly to the BSC by forming a star network.

In star topology the links operate in an independent manner, where the traffic/capacity of the links does not affect each other. Thus, the reliability and the total capacity of the network are increasing compared to the chain topology. Moreover, the capacity can be expanded by adding more links to the base stations that need more bandwidth.

One disadvantage of this network configuration is that it involves a large number of antennas in one place (spatial problem). Additionally, the high number of incoming routes at one point reduces the channel availability.

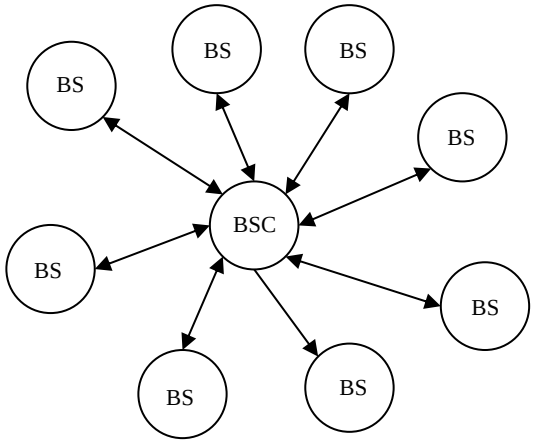

Figure 2.7: Simple Star Topology

2.4.1.3 Ring Topology

Ring topology [11] (Figure 2.8) is a modified version of the chain topology where the BSs have two alternative routes to forward the data without installing additional links. Thus, the reliability of the network is increased.

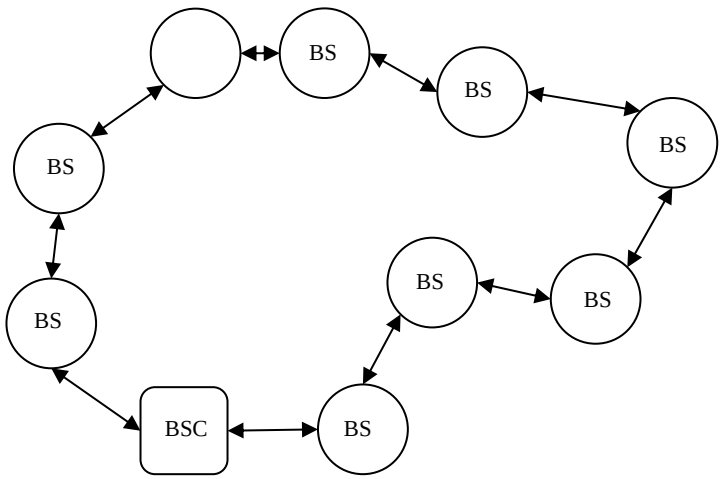

Figure 2.8: Ring Topology

2.4.1.4 Mesh Topology

The mesh topology [11] is a combination of the previous topologies. It is not cost efficient but it increases the network availability and capacity. An example of a mesh topology is depicted in Figure 2.9.

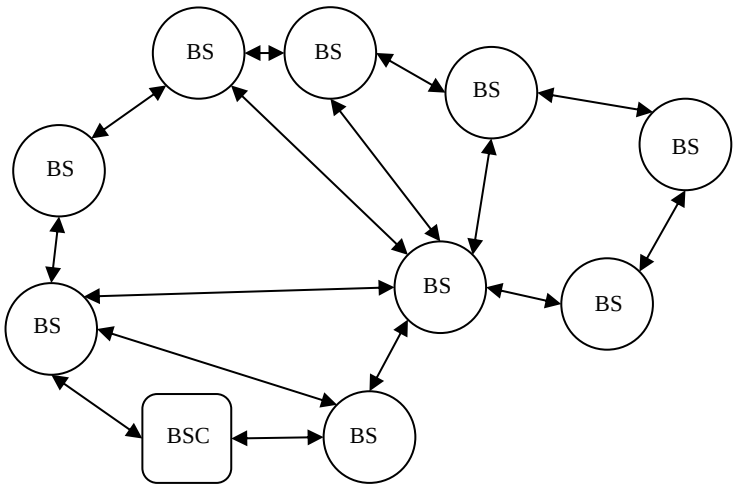

Figure 2.9: Mesh Topology

2.4.2 Link Budget

The maximum distance that the transmitter and the receiver can communicate is limited by the gain and loss factors of the antennas, the transmission lines (feeders), and the propagation conditions (distance, weather conditions) [11]. The link budget calculation is illustrated in Figure 2.10 and can be formulated as:

$$P_R = P_T + G_T + G_R - L_T - L - L_R \; [dB] \qquad (2.5)$$

where P_R is the received signal power, P_T is the transmitted signal power, G_R is the receiver gain, G_T is the transmitter gain, L_R is the receiver branches losses, L_T is the transmitter branches losses and L represents the other losses, such as propagation losses.

After the link budget calculation, the rain fading, the multipath fading, the interference, and other (miscellaneous) losses are analyzed.

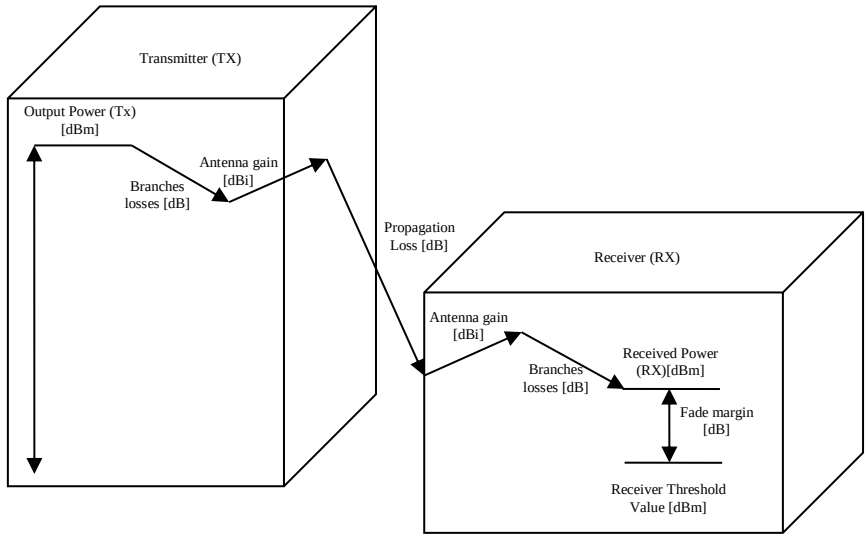

Figure 2.10: Radio Path Link Budget

2.4.3 Fading and Fade Margin

The propagation conditions such as the atmospheric changes and the reflections due to ground/water can cause variations to the received signal [11]. This phenomenon is called fading. The multipath fading is considered when the microwave links are planned. Different types of multipath fading such as the flat fading, the frequency-selective fading, the rain fading, and the refraction-diffraction fading (k-type fading) can significantly affect the quality of the communication by reducing the received signal level. The fading margin is a design allowance that provides sufficient system gain to accommodate the expected fading. This will guarantee the required quality of service in the transmission link.

2.4.4 Automatic Transmit Power Control (ATPC)

As it was mentioned in (2.3.1), in order to compensate for the fading, the power of a transmitter is usually fixed to a higher power level including the fade margin [7]. Of course, during clear sky condition this higher power level can result in increased interference to the other links in MBN.

This problem can be avoided by employing a clever technique that dynamically adjusts the transmit power during fading. Hence, a lower

transmit power level will be utilized during clear sky conditions. Such a solution is referred to as Automatic Transmit Power Control.

The advantages of using ATPC include:

- reduced average power consumption
- extended mean time between failure (MTBF) of equipment
- elimination of the receiver overload phenomenon
- decreased outage due to the reduced influence of adjacent channel interference
- tighter frequency reuse

However, the use of ATPC increases the complexity of the microwave radio system, raises the cost and makes the radio planning process more complicated [12].

If the spectrum is shared between the operators, it will be crucial to coordinate the use of ATPC. This is due to the fact that, if only a subset of the operators utilize ATPC, they will introduce less interference to the other operators, while they themselves may still suffer from the same level of interference. In some countries, the ATPC mode has to be enabled according to the national technical standards.

In ATPC jargon, the following terminology is used [7]:

- Fixed Margin - The margin to the receiver sensitivity threshold during clear sky conditions.
- Dynamic Range - The possible power increase for an ATPC system.

and can be calculated as

$$Fade\ Margin = Fixed\ Margin + Dynamic\ Range \qquad (2.6)$$

The (2.6) is depicted in Figure 2.11.
The ATPC algorithm can be implemented in versatile manners, among which hop-ATPC and node-ATPC are discussed.

2.4.4.1 Hop ATPC

In hop ATPC, the power is regulated individually on every link. In this case, each link based on its propagation conditions will decide which power level should be used depending only on its propagation conditions. Thus, during bad weather conditions, the link will increase the power level in order to compensate for the fading. Nevertheless, the extra power that is used can impose severe interference to the other links.

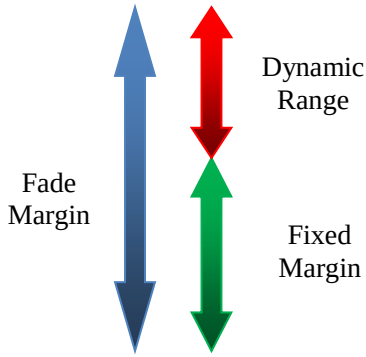

Figure 2.11: The relation between the Fade Margin, Fixed Margin and the Dynamic Range

2.4.4.2 Node ATC

The star topologies are regularly used in dense environments. In section (2.4.1.3), it is mentioned that in star topologies the links are connected to a common node. Applying hop-ATPC to one single link within such a network could introduce and excessive amount of interference to the outer radios.

Assuming that the radios within the center node are coordinated, it is possible to mitigate the excessive interference by increasing the output power levels of unfaded links in accordance with the faded link. In this way, the SINR to the outer radios will be maintained and both the fading the interference will be compensated successfully.

The above mentioned power control technique is known as node-ATPC [15]. Using this technique, any power regulation will be simultaneously applied to all the links that are joined to a common node.

2.4.5 Adaptive Modulation

Depending on the current propagation conditions, the modulation can be dynamically selected [16]. This technique is called adaptive modulation.

The goal of the adaptive modulation is the maximization of the throughput by adjusting the transmission rate to an optimum one given the propagation conditions. A high SINR level permits the use of a high modulation scheme. Thus, the maximum data rates can be achieved during

clear sky conditions. During fading the SINR is decreasing and lower modulation scheme can be applied in order to achieve an acceptable BER.

The modulation scheme can be for example 512-QAM (Quadrature Amplitude Modulation) during clear sky conditions and BPSK (Binary Phase Shift Keying) during heavy rain fading. The real-time voice communication can be named as one of the most important services in cellular networks. The functionality of this service during fading should be guaranteed by the adaptive modulation.

2.5 Antennas

2.5.1 Antenna Parameters

The antennas are devices that transmit and/or receive electromagnetic waves [12]. The antenna characteristics affect significantly the performance of an MBN. The budget link calculation (antenna gain) and the interference level (side lobe level) are potentially influenced by the antenna specifications. The microwave reflector antennas are widely used. This is due to their specific characteristics including:

- high directionality
- high gain
- high radiation efficiency
- narrow beamwidths

The polarization of the electromagnetic radio waves can be utilized to transmit two independent data streams concurrently. The one data stream is using the horizontal component of the wave and the other the vertical component [12]. In this way, tighter frequency reuse is enabled. The polarization could also be used to achieve increased robustness. The Co-Channel Dual Polarized (CCDP) antennas transmit the same data by utilizing both the horizontal and the vertical component of a radio wave. This is due to the fact that the vertical component is not only more resistant to rainfall and other weather disturbances, but also less sensitive to multipath fading [12].

2.5.2 Antenna Models

The radiation masks for the antenna radiation pattern are defined by the radio regulation agencies in order to avoid interference and permit tighter frequency reuse [12].

The two major radio regulation agencies are the FCC in US and the ETSI in Europe. The regulation agencies define the Radiation Pattern Envelope (RPE) for specific frequency band and the associated performance classes. Figures 2-12 – 2.14 represent the ETSI provided RPEs in the frequency range of 14-20 GHz and for class 2, class 3 and class 4 respectively.

The tables 2.1, 2.2 and 2.3 summarize the information of Figures 2.12-2.14. These tables are utilized in order to evaluate the performance of the power control algorithms.

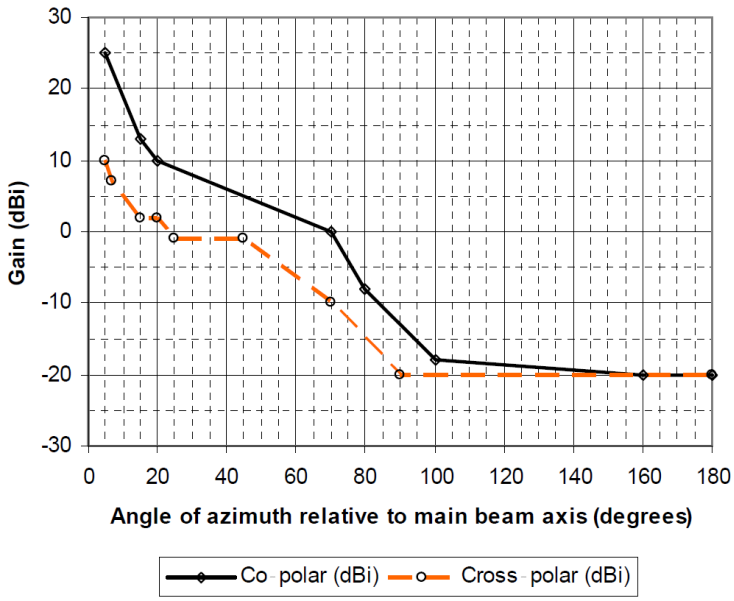

Figure 2.12: Class 2 RPE [17]

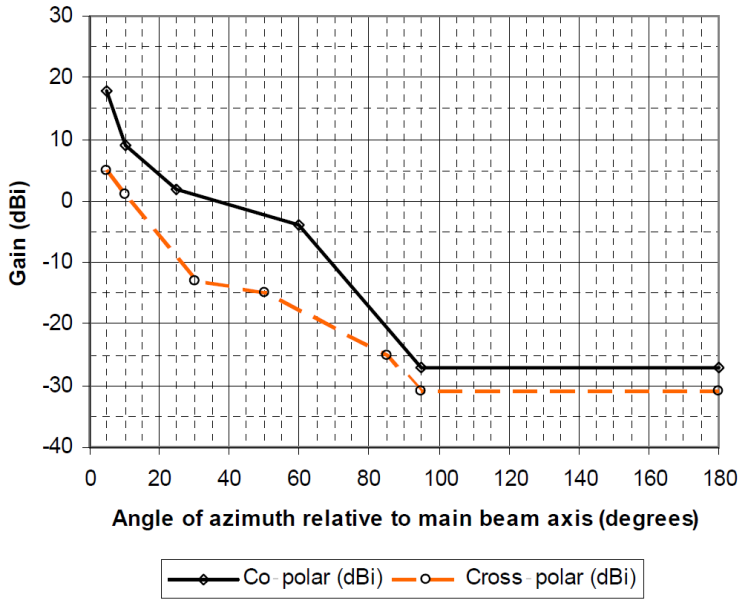

Figure 2.13: Class 3 RPE [17]

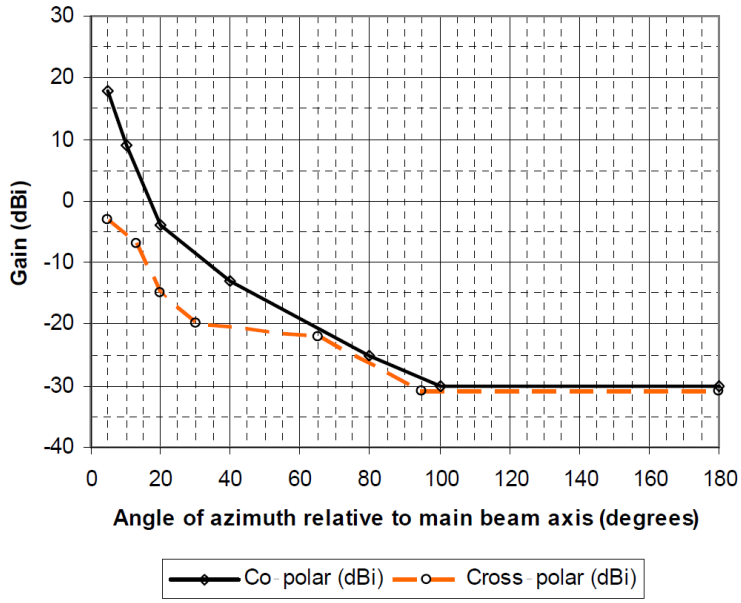

Figure 2.14: Class 4 RPE [17]

Table 2.1: Class 2 RPE [17]

Angle (°)	Co-polar (dBi)	Angle (°)	Cross-polar (dBi)
5	25	5	10
15	13	7	7
20	10	15	2
70	0	20	2
80	-8	25	-1
100	-18	45	-1
160	-20	70	-10
180	-20	90	-20
		180	-20

Table 2.2: Class 3 RPE [17]

Angle (°)	Co-polar (dBi)	Angle (°)	Cross-polar (dBi)
5	18	5	5
10	9	10	1
25	2	30	-13
60	-4	50	-15
95	-27	85	-25
180	-27	95	-31
		180	-31

Table 2.3: Class 4 RPE [17]

Angle (°)	Co-polar (dBi)	Angle (°)	Cross-polar (dBi)
5	18	5	-3
10	9	13	-7
20	-4	20	-15
40	-13	30	-20
80	-25	65	-22
100	-30	95	-31
180	-30	180	-31

2.6 Losses and Attenuation

The three main factors that contribute to the loss/attenuation are the following:

- propagation losses are caused by the Earth's atmosphere and terrain, and include free-space path loss, gas absorption, vegetation attenuation, precipitation (mainly rain), ground reflection, and obstacles.
- branching losses come from the transmission/receiving hardware e.g., waveguides as well as splitters and attenuators.
- "miscellaneous" losses are caused by unpredictable and sporadic factors, such as sand and dust storms, fog, clouds, smoke, and moving objects crossing the path. Poor equipment installation and imperfect antenna alignment can further contribute to the losses. The miscellaneous losses are usually accounted as a part of the fading margin.

2.6.1 Free Space Path Loss

The signal attenuation between two geometrically separated points that have a clear, unobstructed line-of-site path between them is described by the free-space path loss (FSPL) model [11].

The FSPL attenuation is directly proportional to the square of distance and frequency and when two isotropic antennas are used is expressed in absolute numbers by the following equation:

$$FSPL = \left(\frac{4\pi d}{\lambda}\right)^2 \tag{2.7}$$

where $d\,[m]$ is the distance between the transmit and receive antennas, $\lambda\,[m]$ is the operating wavelength, and $c\,[m/s]$ is the speed of light in vacuum.

2.6.2 Fresnel Zone

In microwave point-to-point communication the line of sight is required. However, signal attenuation is caused by obstructions (such as terrain, vegetation, buildings, and others) that penetrate the Fresnel zone [11]. Fresnel zones are elliptically shaped three-dimensional volumes surrounding the main direction of the LOS radio path [12].

The higher the transmission frequency, the narrower the Fresnel zone is [11]. The LOS clearance is mainly defined by the first Fresnel zone, which is depicted in the Figure 2.15. The radius of the n^{th} Fresnel zone is approximated by:

$$R_n = \sqrt{\frac{n\lambda d_1 d_2}{f(d_1 + d_2)}} \tag{2.8}$$

where n is the Fresnel zone number, $\lambda\,[m]$ refers the transmission wavelength, d_1 and d_2 $[km]$ are the distances from the link's antennas, and f is the carrier frequency in $[GHz]$.

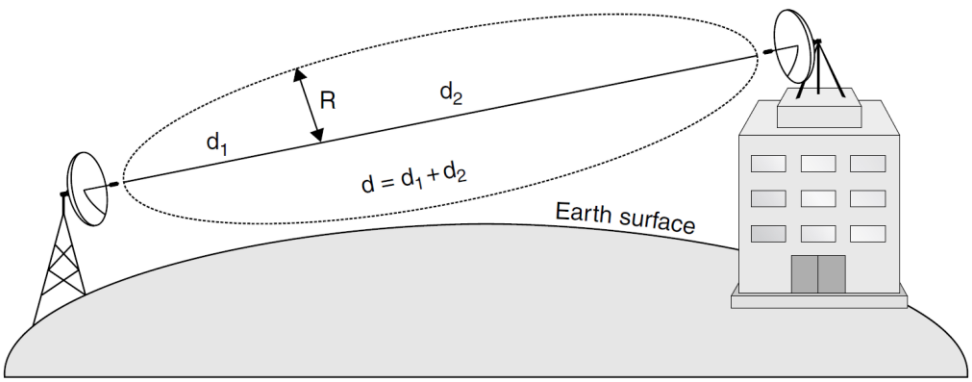

d = Distance between antennas (hop length in kilometers)
R = First fresnal zone radius in meters
f = Frequency in Gigahertz

Figure 2.15: First Fresnel Zone illustration [11]

2.6.3 Vegetation Attenuation

As it was mentioned in (2.6.1), the microwave point-to-point transmission requires LOS path between the base stations as well as clear Fresnel zone (first zone) [11]. The vegetation can cause significant attenuation and factors such as the growing vegetation rate must be considered during microwave planning. In order to avoid the unexpected obstacle attenuation, high-resolution path profiles and careful site and path surveys are used. In the case that the vegetation is continuous, it is important to ensure that MBN will be operational for at least the next ten years.

The millimeter-wave frequencies are affected significantly by the foliage. For the case in which the foliage depth is less than 400 m, according to the CCIR Report 236-2, the attenuation is given by:

$$L = 0.2 f^{0.3} d^{0.6} \, [dB] \tag{2.9}$$

where f $[MHz]$ the operational frequency and d $[m]$ refers to the foliage depth. The relationship (2.9) is applicable for frequency range of 200 $[MHz]$ – 95 GHz.

2.6.4 Gas Absorption

The medium of the microwave transmission is the real atmosphere and not the free space. The total volume of the atmosphere is consisted mostly (99%) by nitrogen and oxygen molecules. The presence of nitrogen is not affecting the microwave radio communications as its absorption bands are located far from the microwave spectrum. Gas absorption, therefore, can be associated with both dry air (oxygen molecules) and water vapor (water molecules). The absorption peak of the water molecules is around 23 GHz and of the oxygen molecules is around 60 GHz. The attenuation that is caused by the atmosphere (dB/km) is calculated as the sum of water vapor and oxygen attenuation. The atmosphere attenuation is strongly dependent on the frequency, as it is show in Figure 2.16.

2.6.5 Precipitation Attenuation

The weather conditions (rain, snow, hail, fog, and haze) can cause precipitation attenuation, which depends on the size and form of their water drops. The frequency range that is used by the commercial radio links is mostly affected by the rain attenuation [11].

Rain attenuation increases with frequency and becomes a major contributor in the frequency bands above 10 GHz.

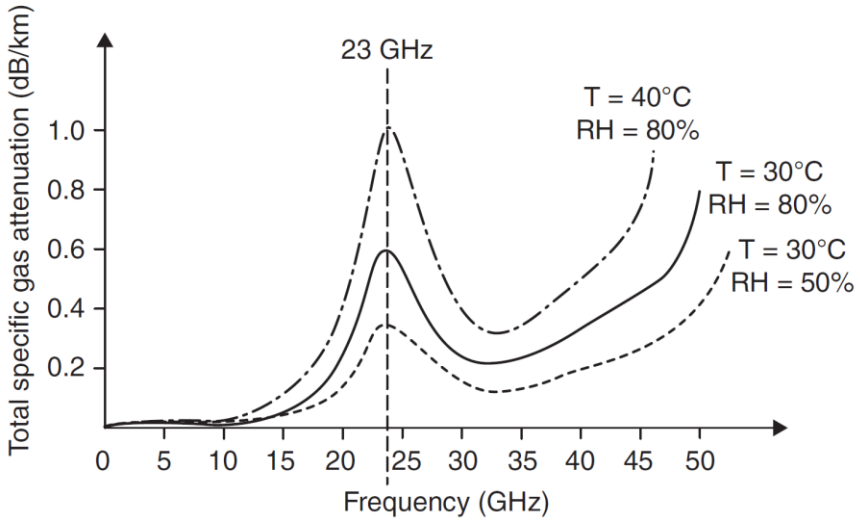

Figure 2.16: Gas attenuation versus frequency [11]

The main parameters used in the calculation of rain attenuation are the form and the size distribution of the raindrops, the polarization, the rain intensity, and the transmission frequency. The contribution of rain attenuation is not included in the link budget and is only accounted for the calculation of rain fading.

It is important to notice that rain attenuation increases exponentially with rain intensity (mm/hr) and that horizontal polarization gives more rain attenuation than vertical polarization.

2.6.6 Diffraction Loss

The diffraction loss is caused by the obstacles present to the LOS path that connects the microwave radios [11]. The attenuation is depending on the shape, size, and properties of the obstacle.

One simple method that is used for the calculation of the obstacle loss is the single-peak method, which is based on the knife-edge approximation [11]. The knife-edge diffraction modeling is illustrated in Figure 2.17.

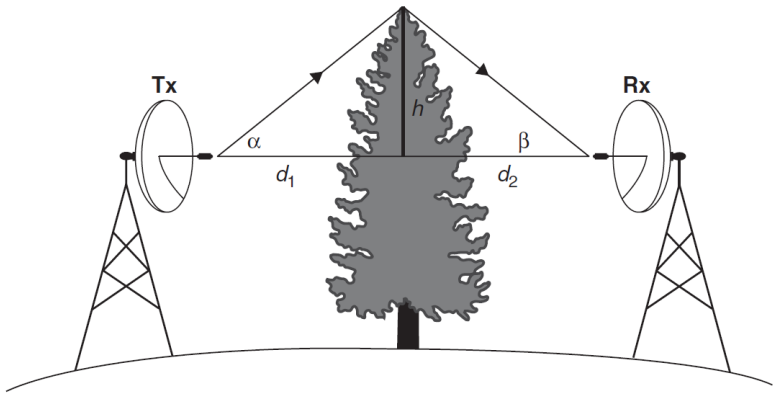

Figure 2.17: Knife-edge diffraction modeling [11]

The methodology for the calculation of the diffraction loss is described in Appendix A.1. Other methods for calculating the diffraction attenuation are described [18] (ITU-R propagation models).

2.6.7 Ground Reflection

The ground reflection can cause attenuation to the received signal because of multipath propagation [11]. The received signal strength is depending on the path geometry: the total reflection coefficient of the ground, and the phase shift.

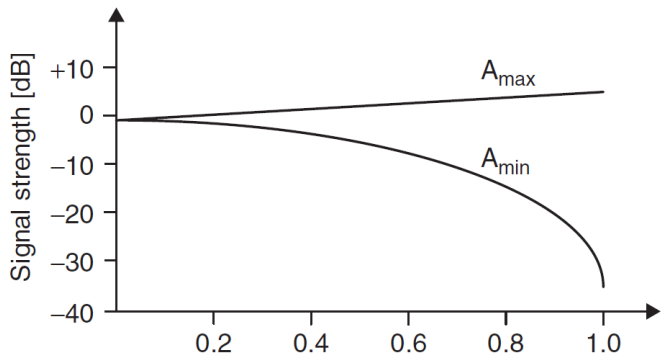

Figure 2.18: Total reflection coefficient [11]

Figure 2.18 illustrates the signal gain/loss as a function of the total reflection coefficient. The maximum gain is obtained for a phase angle of 0° and the maximum loss for a phase angle of 180°.

2.6.8 Atmospheric Stratification

Depending on meteorological conditions, the atmosphere may contain several layers each of which may have different refractivity index. This condition, which is called stratification and is more probable during summer, can result in multipath fading [11].

2.7 Interference

The interference between systems that are using adjacent frequencies is an important issue to be considered [11]. CIR value defines the capability of the receiver to successfully decode the wanted signal when the interference is present. In order to maintain an acceptable level of BER, the CIR is required to be maintained at a high level. There are three main types of interference in a radio system:

- *Co-channel interference*: both the interfering signal and the wanted signal are using the same frequency and polarization. The receiver has a required CIR, which is called co-polar discrimination.
- *Cross-polar interference*: both the interfering signal and the wanted signal are using the same frequency but different polarization. The receiver has a required minimum required CIR, which is called cross-polar discrimination.
- *Adjacent channel interference*: a receiver is usually designed to be protected against the interference produced by the adjacent channels (higher or lower frequencies). The system can be operational for a minimum CIR, which is called the adjacent channel discrimination.

Typically, the co-polar discrimination requires higher levels of CIR compared to cross-polar and adjacent channel interference. During the frequency planning process, the co-polar interference sensitivity is considered and it can be eliminated using an optimum frequency deployment.

2.7.1 Interference Suppression Techniques

2.7.1.1 Cross-Polarization Interference Cancellation (XPIC)

The orthogonal polarization can be used to transmit two data streams on the same radio frequency. This means two signals are transmitted utilizing

the orthogonal and the vertical polarization of the electromagnetic field. Supposing that the cross-polar discrimination (XPD) is sufficient for interference-free transmission, the capacity can be doubled by transmitting two separate, data streams.

In reality, the XPD is imperfect and the interference level in the channel rises and may cause signal quality degradation and errors in the data traffic. The XPD can be increased by using the XPIC technology. Using the XPIC, the performance of the system is limited by the co-polar attenuation rather than the cross-polar interference.

2.7.1.2 Node Cancellation

Given that the interfering signal strength is sufficiently weaker than the wanted signal, the XPIC technique can also be used to reduce the co-channel interference [15]. The prerequisite for this method, which is known as node cancellation, is that the interfering signal is available and accessible.

CHAPTER 3

3 Power Control Optimization

In this chapter, the power control technique using the convex optimization technique is analyzed.

3.1 Introduction

MBNs are peer-to-peer networks where the links are sharing a specific spectrum. In such networks, the co-channel interference is present and limits both the performance and the frequency reuse capability. The purpose of using dynamic power control algorithms instead of using a fixed power level is to enable a tighter frequency reuse. The Quality of Service (QoS) level of the microwave links is captured by utility functions that depend on the received SINR [2].

The adaptive power control algorithm defines dynamically the transmitting power level of each link in order to satisfy the QoS requirements. In the following sections, a sum-utility maximization problem, subject to maximum and minimum utility (or SINR) constraints, is solved to find the optimum power control scheme.

3.2 Assumptions and Notation

It is assumed that an MBN is consisted by M pairs of radios (M peer-to-peer communication links), which are using the same frequency band. Every link $i \in M$ of the network has one transmitter Tx_i and one receiver Rx_i.

The path gain between the transmitter of the link i and the receiver of the link j is denoted by h_{ij}. The noise level at receiver Rx_i is expressed as n_i and the transmission power of the transmitter Tx_i is indicated as p_i. The transmission power is bounded by an upper value p_i^{max}, $0 \leq p_i \leq p_i^{max}$. The SINR level at receiver Rx_i is given by:

$$\gamma_i := \frac{h_{ii} p_i}{n_i + \sum_{k \neq i} h_{ki} p_k} \tag{3.1}$$

The notation is summarized in table 3.1.

Table 3.1: Notation of the power control problem variables

Parameter	Notation
Number of links	M
Channel gain	h_{ij}
Noise	n_i
Transmission power	p_i
Maximum transmission power	p_i^{max}
SINR	γ_i

3.3 Problem parameters

3.3.1 Utility Function

The utility function is associated with each link $i \in M$ and is expressed by the generic function $u(\gamma_i)$. The goal is to maximize the utility function $u(\gamma_i)$ for all the links of the network. If the utility function is strictly increasing (monotonic) and continuous [2], then the function's constraints map one-to-one to the SINR bounds. In this case:

$$u_i(\gamma_i) \in \left[u_i(\gamma_i^{min}), u_i(\gamma_i^{max})\right] \Leftrightarrow \gamma_i \in \left[\gamma_i^{min}, \gamma_i^{max}\right] \tag{3.2}$$

The lower bounds ensure that a minimum QoS level will be kept while the upper bounds ensure that the available resources will be used in a proper way e.g. limited power level that can be handled at the receiver.

According to the Shannon capacity theorem [19], the theoretical upper bound on the communication rate through an additive white Gaussian noise channel is:

$$C_i := B_i log_2(1 + \gamma_i) \tag{3.3}$$

where C_ι is the channel capacity in bits per second $[bps]$ and B_i is the bandwidth of the channel in Hertz $[Hz]$.

The utility function $u(\gamma_i)$ can represent the quantity that is desired to be maximized e.g. rate. Furthermore, the utility function could be chosen in a way that the maximization problem could be easily converted to a convex one through reformulation. The logarithmic function has the properties, which can fulfill the aforementioned criteria. Thus, in the following sections the utility function $u(\gamma_i) = \ln(\gamma_i)$ will be used to mathematically formulate the optimized power control problem.

3.3.2 Power Consumption

The green communication has attracted a lot of attention in recent years. As a consequence, lower power consumption can be viewed on a critical criterion in radio link designs. In current study this issue is considered and hence the power control problem is optimized with respect to the total power consumption. The total power consumption is defined as the sum of the power levels consumed by all the links of MBN and is minimized under the following statement: $\min_{0 \le p_i \le p^{max}} \sum_{i=1}^{M} p_i$.

3.4 Optimization problem

Concluding the above mentioned criteria regarding the utility and power consumption issues, the power control optimization problem can be defined as:

$$Problem: \max_{\mathbf{0} \le \boldsymbol{p} \le \boldsymbol{p^{max}}} \sum_{i=1}^{M} u_i(\gamma_i) + \min_{\mathbf{0} \le \boldsymbol{p} \le \boldsymbol{p^{max}}} \sum_{i=1}^{M} p_i \qquad (3.4a)$$

$$Subject\ to: \gamma_i^{min} \le \gamma_i \le \gamma_i^{max}, \forall\, i \in M \qquad (3.4b)$$

where $\boldsymbol{p} := [p_1, \dots, p_M]^T$ and $\boldsymbol{p_{max}} := [{p_1}^{max}, \dots, {p_M}^{max}]^T$. The first term of $(3.4a)$ expresses the maximization of the utilization of the network, while the second term refers to the minimization of the power consumption. The bounds of the SINR level at $(3.4b)$ express the QoS constraints of the network links. The use of the low SINR bound γ_i^{min} will guarantee that the SINR level at link i will be at least γ_i^{min} and the link will be operational.

This is while the upper SINR bound is used to ensure that the maximum SINR level will not exceed γ_i^{max}, which is prescribed by the hardware limitations or SINR level defined by QoS.

This power control problem formulation allows the network to have diverse range of QoS levels. That is very common when the links of the network utilize different hardware equipment or have different SINR requirements. By this, the links, which are more critical for the network stability, can be set to have stricter QoS requirements.

The problem (3.4a) is convex, and therefore will be first reformulated applying suitable relaxation methods.

3.5 Efficient optimization through convex relaxation

3.5.1 Assumptions

In order to obtain an efficient solution for the problem (3.4a), three assumptions are adopted:

Assumption 1 [2]: The utility function $u_i(\gamma_i)$ is strictly increasing and twice continuously differentiable. Furthermore, the following statement is valid:

$$\frac{-\gamma_i \frac{d^2 u_i(\gamma_i)}{d\gamma_i^{\,2}}}{\frac{du_i(\gamma_i)}{d\gamma_i}} \geq 1 \quad for\ \gamma_i > 0 \tag{3.5}$$

The above assumption [23] is commonly addressed in power control literatures and implies that the utility function $u_i(\gamma_i)$ is strictly concave in γ_i. Moreover, for lower values of SINR, it leads to $\lim_{\gamma_i \to 0+} u_i(\gamma_i) = -\infty$ by which non-zero power allocation to all the links is guaranteed. The constraints of (3.4b) only require the utility function to be monotonic. The abovementioned requirements can be fulfilled by $u(\gamma_i) = \ln(\gamma_i)$, which was selected as utility function in (3.3.1).

Assumption 2 [2]: The noise power is non-zero for all links i.e. $n_i > 0$ for all $i \in M$, and the gain matrix $\boldsymbol{A} = [a_{ij}]$, $a_{ij} := {}^{h_{ji}}\!/_{h_{ii}}$ is irreducible and cannot be decomposed into smaller problems of the same type [24].

This assumption is also a standard assumption in power control problems.

Assumption 3 [2]: If every user has a maximum SINR constraint, there is no power vector $\widetilde{\boldsymbol{p}}$ with $\boldsymbol{0} < \widetilde{\boldsymbol{p}} \leq \boldsymbol{p^{max}}$ such that the resulting SINRs $\widetilde{\boldsymbol{\gamma}}$ satisfy $\widetilde{\boldsymbol{\gamma}} = \boldsymbol{\gamma^{max}}$ for all $i \in M$.

Assumption 3 is applied in the case that all the users have maximum SINR constraints. If a vector $\widetilde{\boldsymbol{p}}$ exists then there is no reason for optimization as the $\widetilde{\boldsymbol{p}}$ would be the optimal solution for the power control problem. Assumption 3 is automatically satisfied when there is no upper QoS bound i.e when $\gamma_i^{max} = \infty$.

3.5.2 Convex Relaxation

Having clarified the operating conditions in 3.5.1, the problem (3.4) can be relaxed by introducing an auxiliary variable q_i. The variable q_i, which is associated to each link i, will provide an upper bound for the interference-plus-noise (IpN) term $n_i + \sum_{k \neq i} h_{ki} p_k$ [2]. The relaxed version of (3.4) then can be reformulated as:

$$Problem: \max_{\boldsymbol{0} \leq \boldsymbol{p} \leq \boldsymbol{p^{max}},\ \boldsymbol{q} \in \mathbb{R}^M_{++}} \sum_{i=1}^{M} u_i(h_{ii} p_i q_i^{-1}) + \min_{\boldsymbol{0} \leq \boldsymbol{p} \leq \boldsymbol{p^{max}}} \sum_{i=1}^{M} p_i \qquad (3.6a)$$

$$Subject\ to: \gamma_i^{min} \leq h_{ii} p_i q_i^{-1} \leq \gamma_i^{max}, \forall\ i \in M \qquad (3.6b)$$

$$n_i + \sum_{k \neq i} h_{ki} p_k \leq q_i\ , \forall\ i \in M \qquad (3.6c)$$

where $\boldsymbol{q} := [q_1, \dots, q_M]^T$.

In [2] it is shown that the problems (3.4) and (3.6) are equivalent. Consequently, the problem is converted to a convex one by setting the

variables p_i and q_i to $p_i = e^{y_i}$ and $q_i = e^{z_i}$ respectively, and can be rewritten as:

$$Problem: \max_{-\infty < \boldsymbol{y} \le \ln \boldsymbol{p^{max}},\ \boldsymbol{z} \in \mathbb{R}^M_{++}} \sum_{i=1}^{M} u_i\left(\frac{h_{ii}e^{y_i}}{e^{z_i}}\right) + \min_{\boldsymbol{0} \le \boldsymbol{p} \le \boldsymbol{p^{max}}} \sum_{i=1}^{M} e^{y_i} \qquad (3.7a)$$

$$Subject\ to: p_i^{min} e^{-y_i} \le 1, \forall\ i \in M \qquad (3.7b)$$

$$(p_i^{max})^{-1} e^{y_i} \le 1, \forall\ i \in M \qquad (3.7c)$$

$$\gamma_i^{min} {h_{ii}}^{-1} e^{z_i - y_i} \le 1\ , \forall\ i \in M \qquad (3.7d)$$

$$\gamma_i^{max^{-1}} h_{ii} e^{y_i - z_i} \le 1\ , \forall\ i \in M \qquad (3.7e)$$

$$n_i e^{-z_i} + \sum_{k \ne i} h_{ki} e^{y_k - z_i} \le 1\ , \forall\ i \in M \qquad (3.7f)$$

where $\boldsymbol{y} := [y_1, \dots, y_M]^T$, $\boldsymbol{z} := [z_1, \dots, z_M]^T$, $\mathbb{R}_{++}$ denotes the positive reals and $-\infty < \boldsymbol{y} \le \ln \boldsymbol{p^{max}}$ defines both the lower and the upper bound for the power transmission level when the exponential function is used for the convex transformation of the problem.

The transformed constraints are convex since all the left hand sides ($3.7b$ – $3.7f$) are compositions of non-negative sums of exponential functions [2, 25]. The same conclusion is valid for ($3.7a$) as it consists of a nonnegative sum of concave utility functions $u_i(e^x) = u_i(e^{y_i - z_i + \ln(h_{ii})})$ and sum of power levels in exponential form. According to the assumption 1, the utility function must also fulfill the following inequality:

$$\frac{-\xi \dfrac{d^2 u_i(\xi)}{d\xi^2}}{\dfrac{du_i(\xi)}{d\xi}} \ge 1 \quad for\ \xi = e^x \qquad (3.8)$$

The inequality (3.8) is satisfied when the natural logarithmic function is employed as the utility function.

3.6 Power allocation using Lagrange multipliers

3.6.1 Lagrangian Function

Let ν_i, λ_i, μ_i denote the Lagrange multipliers corresponding to the minimum and maximum SINR ($3.7d$ - $3.7e$) and local IpN ($3.7f$) constraints. The Lagrangian function of the convex equivalent problem (3.7) is:

$$L(\boldsymbol{y},\boldsymbol{z},\boldsymbol{\nu},\boldsymbol{\lambda},\boldsymbol{\mu}) = -\sum_i u_i\left(\frac{h_{ii}e^{y_i}}{e^{z_i}}\right) + \sum_i e^{y_i} + \sum_i \nu_i\left(\gamma_i^{min}{h_{ii}}^{-1}e^{z_i-y_i} - 1\right) + \sum_i \lambda_i\left(\gamma_i^{max^{-1}}h_{ii}e^{y_i-z_i} - 1\right) + \sum_i \mu_i\left[e^{-z_i}\left(n_i + \sum_{k\neq i} h_{ki}y_k\right) - 1\right] \quad (3.9)$$

where $\boldsymbol{\nu} := [\nu_1, \dots, \nu_M]^T$, $\boldsymbol{\lambda} := [\lambda_1, \dots, \lambda_M]^T$ and $\boldsymbol{\mu} := [\mu_1, \dots, \mu_M]^T$.

3.6.2 Gradient Descent Method

Employing the Gradient Descent Method [Appendix A.2], (3.9) can be solved as follows:

$$y_i(t+1) = \left[y_i(t) - \beta\nabla_{y_i}L(\omega(t))\right]_{y_i} \quad (3.10a)$$

$$z_i(t+1) = z_i(t) - \beta\nabla_{z_i}L(\omega(t)) \quad (3.10b)$$

$$\nu_i(t+1) = \left[\nu_i(t) + \beta\nabla_{\nu_i}L(\omega(t))\right]^+ \quad (3.10c)$$

$$\lambda_i(t+1) = \left[\lambda_i(t) + \beta\nabla_{\lambda_i}L(\omega(t))\right]^+ \quad (3.10d)$$

$$\mu_i(t+1) = \left[\mu_i(t) + \beta \nabla_{\mu_i} L(\omega(t))\right]^+ \quad (3.10e)$$

where $\omega := \{\boldsymbol{y}, \boldsymbol{z}, \boldsymbol{\nu}, \boldsymbol{\lambda}, \boldsymbol{\mu}\}$ β is the constant step size and $[x]^+ = \max\{0, x\}$. Applying (3.10) on (3.9) and including the maximum power limitation at $(3.10a)$, the solution of the problem (3.7) is the following:

$$y_i(t+1) = min\left\{y_i(t) - \beta \frac{\partial L(\boldsymbol{\omega})}{\partial y_i}\bigg|_{\boldsymbol{\omega}(t)}, y_i^{max}\right\} \quad (3.11a)$$

$$z_i(t+1) = z_i(t) - \beta \frac{\partial L(\boldsymbol{\omega})}{\partial z_i}\bigg|_{\boldsymbol{\omega}(t)} \quad (3.11b)$$

$$\nu_i(t+1) = \left[\nu_i(t) + \beta\left(\frac{\gamma_i^{min} e^{z_i(t)-y_i(t)}}{h_{ii}} - 1\right)\right]^+ \quad (3.11c)$$

$$\lambda_i(t+1) = \left[\lambda_i(t) + \beta\left(\frac{h_{ii} e^{y_i(t)-z_i(t)}}{\gamma_i^{max\chi}} - 1\right)\right]^+ \quad (3.11d)$$

$$\mu_i(t+1) = \left[\mu_i(t) + \beta\left(e^{-z_i(t)}\left(n_i + \sum_{k\neq i} h_{ki} e^{y_k(t)}\right) - 1\right)\right]^+ \quad (3.11e)$$

where

$$\frac{\partial L(\boldsymbol{\omega})}{\partial y_i} = -\frac{du_i\left(\frac{h_{ii}e^{y_i}}{e^{z_i}}\right)}{dy_i}\frac{h_{ii}e^{y_i}}{e^{z_i}} + e^{y_i} + e^{y_i}\sum_{j\neq i} h_{ij}\mu_j e^{-z_j} + \frac{\lambda_i}{\gamma_i^{max}}\frac{h_{ii}e^{y_i}}{e^{z_i}} - \nu_i\gamma_i^{min}\frac{e^{z_i}}{h_{ii}e^{y_i}} \quad (3.12a)$$

$$\frac{\partial L(\boldsymbol{\omega})}{\partial z_i} = \frac{du_i\left(\frac{h_{ii}e^{y_i}}{e^{z_i}}\right)}{dy_i}\frac{h_{ii}e^{y_i}}{e^{z_i}} - \mu_i e^{-z_i}\left(n_i + \sum_{k\neq i} h_{ki}e^{y_k}\right) - \frac{\lambda_i}{\gamma_i^{max}}\frac{h_{ii}e^{y_i}}{e^{z_i}} + \nu_i\gamma_i^{min}\frac{e^{z_i}}{h_{ii}e^{y_i}} \quad (3.12b)$$

CHAPTER 4

4 Methodology

In the initial part of this chapter, the system setup, the case study and the frequency deployment algorithms are explained and analyzed. Moreover, the antenna models, the assumptions and the parameters used in the implementation of the simulator are described and motivated.

4.1 System Setup

In [1], six different system setups have been simulated, evaluated and compared. Optimized-ATPC will be compared with the two best-performance setups of [1] including node ATPC, with and without node cancellation.

It is expected that the performance of optimized-ATPC will be better in terms of spectrum efficiency and network utilization. Optimized-ATPC does not use any interference cancellation technique due to the fact that interference cancellation did not found to improve the spectral efficiency [section 5.4].

4.2 Case study

The purpose of using dynamic power control algorithms instead of using a fixed power level is to enable a tighter frequency reuse. The SINR level of the receivers in an MBN must exceed a specific value for a reliable communication. This value varies depending on both the receiver type and the modulation scheme that are used. Given a fixed MBN topology and a frequency deployment scheme, it is possible that the requirement for a specified SINR level is violated. Then, either the interference in MBN has to be reduced or the frequency deployment has to be altered.

A tighter frequency reuse can be enabled by keeping the same frequency to as many links as possible. In [1], node cancellation and node ATPC

techniques are used to achieve an acceptable level of SINR and to reduce the total number of frequencies that are required for MBN operation.

The basic microwave network topology that will be used to describe the power control optimization technique is illustrated in Figure 4.1. In this MBN, the first microwave link includes the radios 1 and 2 and the second microwave link consists of the radios 3 and 4. The solid lines represent the wanted signals and the dashed lines are the interfering signals.

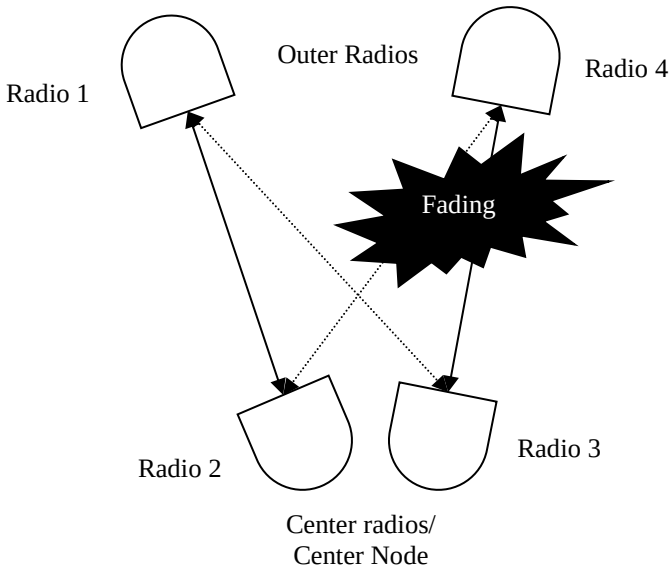

Figure 3.1: Case study using two links

As it can be found from the figure, the link between the radios 3 and 4 experiences fading; this can have different impact on different radios. Table 4.1 summarizes the signal and interference impact on the different radios of MBN.

Table 4.1

Radio	**Signal**	**Interference**
1	Unfaded	Unfaded
2	Unfaded	Faded
3	Faded	Unfaded
4	Faded	Faded

The following notation is used in the following chapters:

- Nominal case: the transmission during clear sky conditions (no fading)
- $SINR_{min}$ is the lowest SINR in the system. The $SINR_{min}$ parameter outlines the validity of the frequency deployment setup.
- CIR_{min} is the lowest CIR in the system. The CIR_{min} parameter determines the link with the maximum interference in MBN.

4.3 Analysis of Case Study

In this section, the performance of the power control algorithms under rain fading will be examined.

4.3.1 No ATPC

Considering the case that no ATPC technique is applied, the transmission power level will be fixed to a higher value including the fade margin. Table 4.2 summarizes the effect of rain fading according to the Figure 4.1:

- radio 1: neither the signal nor the interference is faded and the SINR is not affected by the rain fading.
- radio 2: only the interference is faded and the SINR is better than the nominal case.
- radio 3: while the signal is faded, the interference is unfaded and the SINR is lower during rain fading.
- radio 4: both the signal and the interference are faded and the SINR is unchanged compared to the nominal case.

Table 4.2: No ATPC

Radio	**SINR level**
1	$SINR_{nominal} = SINR_{fading}$
2	$SINR_{nominal} < SINR_{fading}$
3	$SINR_{nominal} > SINR_{fading}$
4	$SINR_{nominal} = SINR_{fading}$

4.3.2 Node ATPC

Applying the node-ATPC technique without employing any interference cancellation, the performance of MBN during rain fading is improved and the SINR levels compared to the nominal case are summarized in table 4.3:

- radio 1: it receives more interference because the radio 3 is increasing the power level to compensate for the fading. However, radio 2 is increasing the power according to the radio 3 power amplification and the SINR at radio 1 is the same as in nominal case.
- radio 2: it will not be affected by the power increase of radio 4 as the interference is faded.
- radio 3: it will not be affected by the rain fading as node-ATPC can fully compensate for the signal power level decrease.
- radio 4: it will not be affected by the rain fading as the interference from radio 2 and the signal from radio 3 are equally faded (rain) and increased (ATPC).

Table 4.3: Node ATPC

Radio	SINR level
1	$SINR_{nominal} = SINR_{fading}$
2	$SINR_{nominal} = SINR_{fading}$
3	$SINR_{nominal} = SINR_{fading}$
4	$SINR_{nominal} = SINR_{fading}$

The analysis of the node-ATPC technique assumes that it is possible to compensate fully for the fading. If this is not possible, then interference cancellation techniques could be used to improve the performance of the radios that belong to the center node (node cancellation).

4.3.3 Optimized ATPC

Optimized-ATPC regulates the power level in according with the underlying propagation conditions in order to maximize the network utility and minimize the power consumption of MBN. While node-APTC considers the nominal SINR as the reference to set the target SINR, optimized-ATPC tries to maximize SINR given the propagation conditions. Using optimized-ATPC, it is expected that the nominal SINR will be always higher compared to node-ATPC.

4.4 Node ATPC vs Optimized ATPC

The differences between node-ATPC and optimized-ATPC are summarized in table 4.4.

Table 4.4

Node-ATPC	**Optimized-ATPC**
Distributed power control (node based)	Centralized power control
Assumes communication between the radios belonging to the same center node	Does not assume information exchange between the radios
$SINR_{target} = SINR_{nominal}$	$SINR_{target} = SINR_{maximum}$
Fixed power level during clear sky conditions and limited dynamic range (Figure 2.11)	Fully dynamic power allocation according to the propagation conditions
Topology-depended performance (e.g. Star topology)	Topology-independent performance
Interference Cancellation Techniques	No interference cancellation techniques

The implementation of optimized-ATPC is centralized. The power control unit determines the power level of all the radios of MBN. Assuming that the information on the channel and QoS requirements of MBN are available, it is possible to specify the optimum power level for each individual radio. However, node-ATPC does not require a power control unit that administrates the radios of MBN but it requires communication between the radios that belong to a common node. In this way, the radios that belong to the center nodes exchange information and set their individual power levels in a coordinated way.

The main difference between node-ATPC and optimized-ATPC is that the first aims in an operational MBN under rain fading while the optimized power control aims in an operational MBN with the maximum performance under rain fading. Optimized-ATPC uses the maximum SINR as SINR target that is defined by the hardware limitations of the radios. Thus, it results in an optimal power assignment regardless of propagation conditions. Node-ATPC instead uses the nominal SINR level as SINR target. The nominal SINR is lower or equal to the maximum achievable SINR, resulting in suboptimal network operation.

Moreover, the node-ATPC uses a fixed power level during clear sky conditions by limiting the dynamic range of the power control algorithm. A fixed power level permits the application of interference cancellation techniques, like the node cancellation [1]. However, optimized-ATPC applies a fully dynamic power level range resulting in a low interference level in MBN.

Finally, the performance of the node-ATPC algorithm is strongly dependent on the network topology. The topologies that favor the application of node-ATPC are the joint star network topologies, where multiple radios are connected to a common node and the power control information exchange is feasible. The sub optimality of node-ATPC for random topologies can be compensated by optimized-ATPC as the decisions for the power level depend only on the accuracy of the channel knowledge information.

4.5 Network Scenarios

Several network topologies can be used for the construction of MBNs (section 2.4.1). Three network topologies will be used to evaluate and compare the performance of the power control algorithms.

4.5.1 Simple Star Topology

The star topology is described in section 2.4.4.1. The simple star topology allows information exchange between the radios that are connected to the common node and it is very favorable for the node ATPC and the node cancellation.

The simple star topology that was used during the simulations is depicted in Figure 4.1. Link length of 10 km was used.

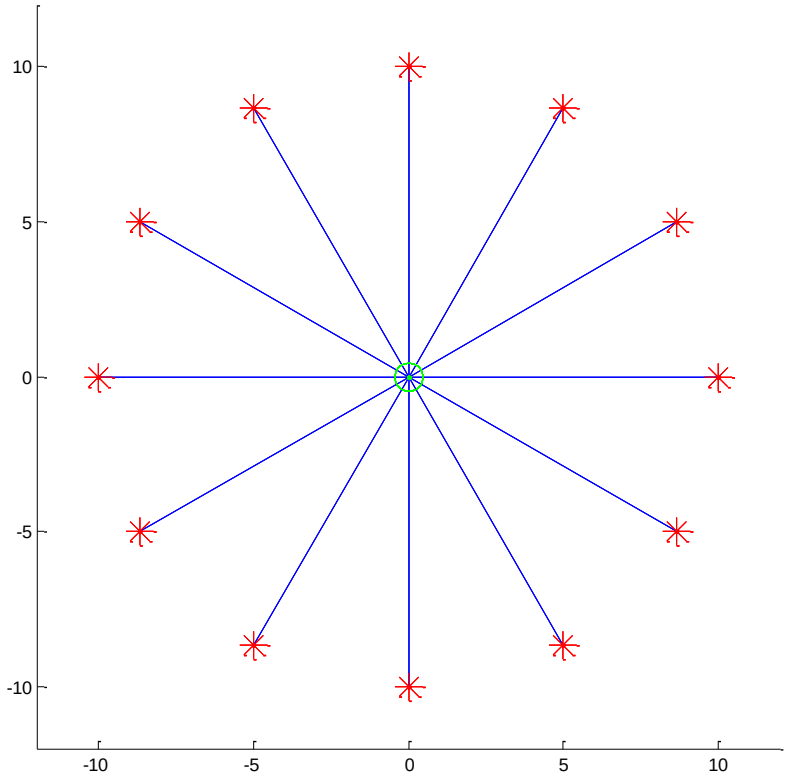

Figure 4.1: Simple Star Topology

4.5.2 4 Joint Stars Topology

The 4-joint star topology includes four simple star topologies each of which consisting 12 links. Each of the links has length of 10km. In case of rain fading, the node ATPC boosts the transmit power in several directions and increases the interference to radios that are not connected to a common node. Thus, the node cancellation cannot compensate for the interference that is caused by the other star topologies. The four star topology is illustrated in Figure 4.2.

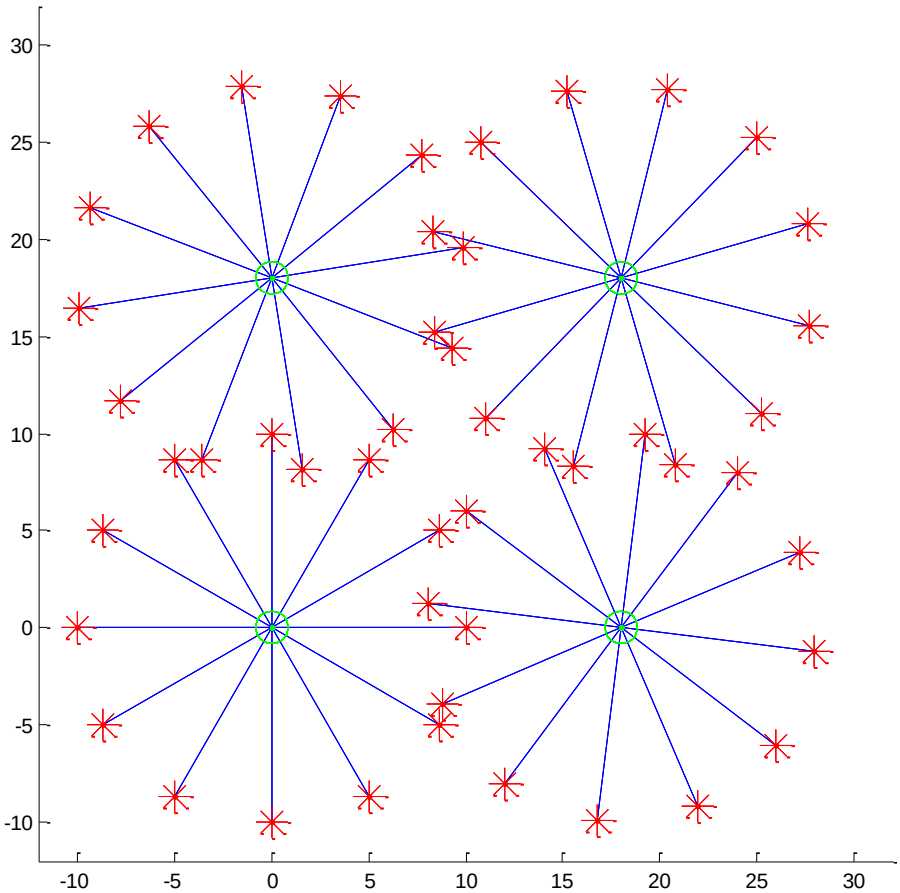

Figure 4.2: 4 Joint Star Topology

4.5.3 Real Network Topology

A real network topology, which approaches the random topology, is used for the evaluation of the power control techniques. The real network is sketched in Figure 4.3 and represents a subset of the Delhi microwave network in India. The link lengths are varying but are typically around 1 km.

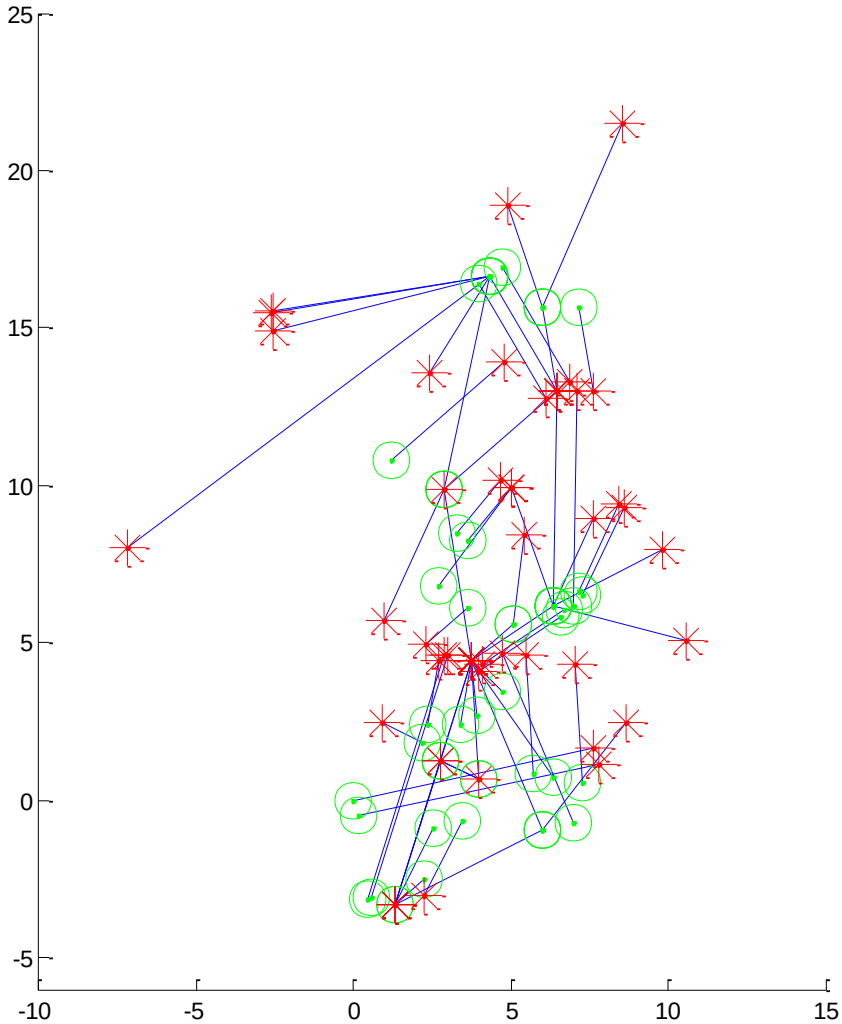

Figure 4.3: Real Network Topology – India

4.6 Models

4.6.1 Antenna Radiation Pattern

Three antenna models are used for the evaluation of the power control algorithms. The main difference between the antennas is the side lobe level (SLL). It should be mentioned that the higher SLL leads to a higher interference level. The antennas used during the simulations are depicted in

Figures 4.4, 4.5 and 4.6. It can be observed that the antenna 1 has the lowest SLLs. The antenna 3 is the worst as it has the strongest SLLs around the mainbeam. Antennas with different SLLs are used to stimulate different levels of the interference within MBN. Testing the power control algorithms with different types of antennas helps in performance evaluation of the algorithms as the interference level potentially affects the frequency reuse capability.

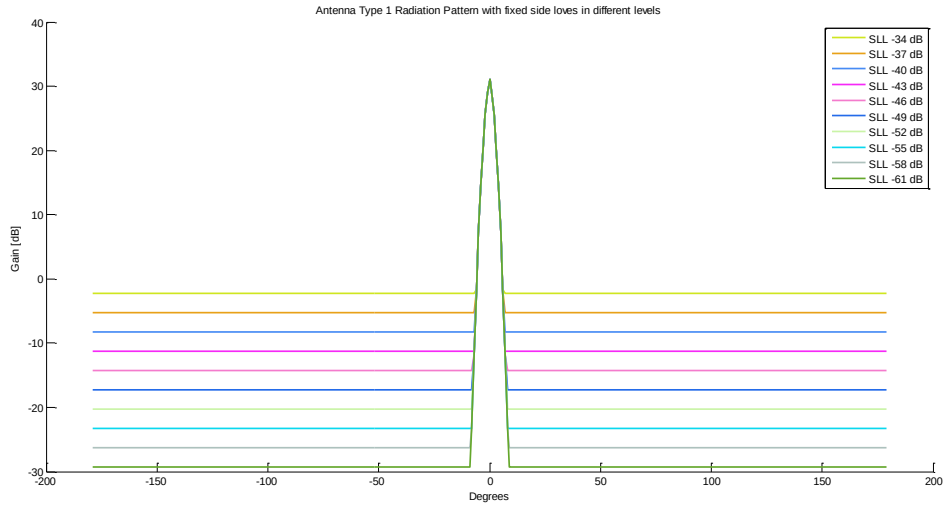

Figure 4.4: Antenna 1 RPE – Fixed SLL example antenna

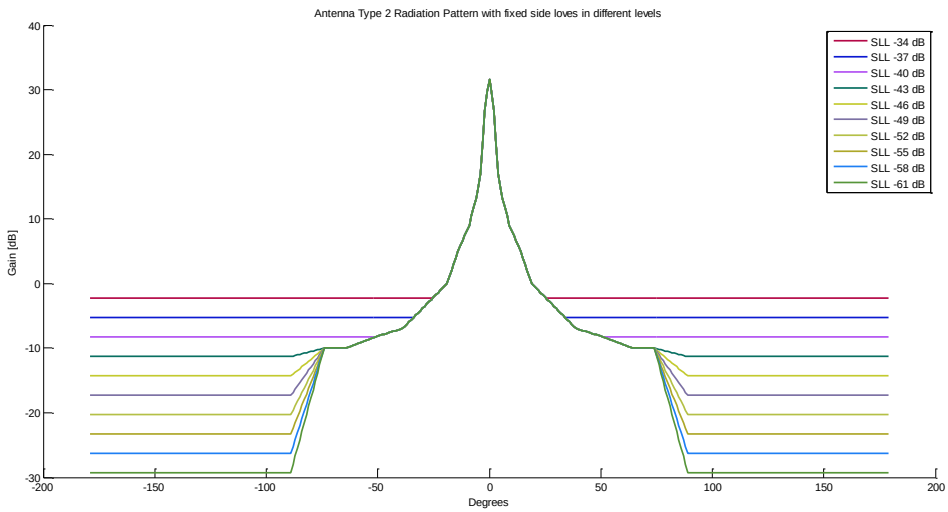

Figure 4.5: Antenna 2 RPE – Modified ETSI with lower SLL

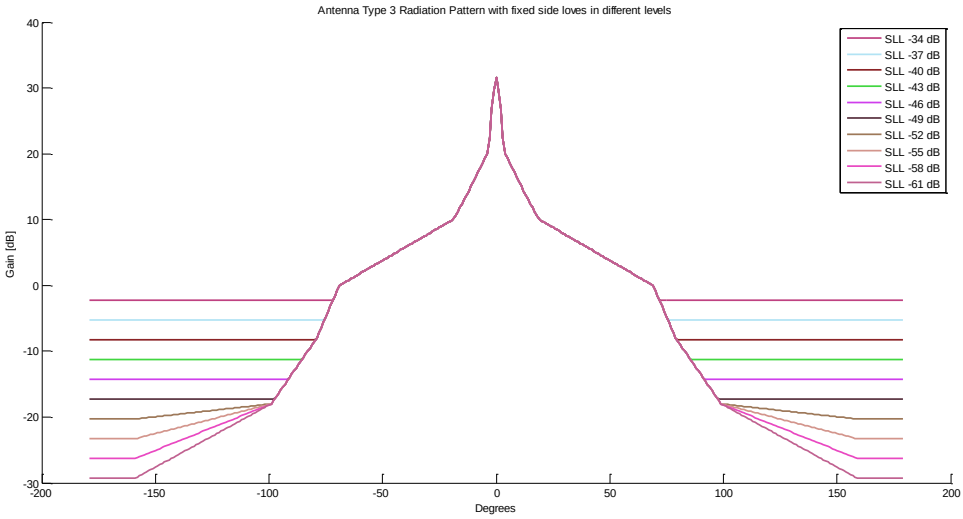

Figure 4.6: Antenna 3 RPE – Modified ETSI with higher SLL

4.6.2 Attenuation

Considering peer to peer wireless communication without the presence of any obstacle, the free space path loss (FSPL) and the rain are main signal attenuation contributors. Both the wanted signal and the interference are subject to FSPL and rain attenuation. According to the recommendation 838 of ITU, the following equation is used to calculate the rain attenuation:

$$\gamma_R = kR^{\alpha} \left[{}^{dB}/_{km} \right] \tag{4.1}$$

where R is the rainfall rate $[mm/hour]$ and the value of parameter a depends on the weather and climatic conditions and it is calculated as follows:

$$k = \frac{k_H + k_V + (k_H - k_V)\cos^2\theta \cos 2\tau}{2} \tag{4.2}$$

$$\alpha = \frac{k_H\alpha_H + k_V\alpha_V + (k_H\alpha_H - k_V\alpha_V)\cos^2\theta \cos 2\tau}{2k} \tag{4.3}$$

where θ is the path elevation angle, τ stands for the polarization angle relative to the horizontal direction and k_H, k_V, α_H, α_V are available in [26].

4.6.3 Rain Model

The rain fading is represented by circular clouds. The clouds have varying diameter and varying rain intensity. For the evaluation of the power control algorithms performance the clouds are moving from one link to another using a round robin scheme. The total wanted signal rain attenuation must be $20dB$ for which (4.1) is used to calculate the radius and the rain density.

The different propagation paths from the transmitters to the receivers are probably affected by the rain fading. The intersection length of the propagation paths with the circular clouds defines the level of rain attenuation. The signal and the interference attenuation levels caused by rain fading are calculated using the equation (4.1) and the respective intersection length.

4.6.4 Interference

During the simulations only the co-channel interference is taken into consideration. The adjacent channel interference is excluded from the interference calculations because otherwise the frequency deployment algorithm becomes complicated. Assuming that the system is using both polarizations for each link, the cross-polar interference is ignored.

4.6.5 Transmitter power

For the initialization of the transmit power, the channel matrix $\boldsymbol{H} = [h_{ij}]$ is used to calculate the minimum power that is needed to transmit a signal through a link. The channel transfer function h_{ij} is calculated according to the link budget scheme (section 2.4.3). Considering that initially the only signal degradation factor in MBN is the noise power n_i and assuming a minimum SINR in each link, the initial power p_{0i} per link is given by:

$$p_{0i} = \frac{SINR_{min} n_i}{h_{ii}} \tag{4.4}$$

with respect to the maximum power p_{max} that can be used by the transmitter. As it was mentioned in section 3.6.2, the initial power state p_{0i} must belong to the solution range. The above power state is valid as it

expresses the minimum power that can be used by MBN and it is not violate the maximum power constraint.

4.6.6 Bit Error Rate

The BER must be kept under a threshold for reliable communication. The required BER level for an operational microwave link is related with the utilized modulation scheme and the minimum SINR. The maximum BER for a certain modulation scheme is given by the manufacturer's hardware datasheet. In the current study, the Mini-Link TN datasheet [27] is used to obtain a proper parametrization.

4.7 Parameters

The parameters of the table 4.5 are used in all the simulations.

Table 4.5: Simulation Parameters

Parameter	Value	Explanation
Frequency	15 $[GHz]$	Frequency used by the simulated network
Maximum Transmitter Power	30 $[dBm]$	[27]
Minimum Transmitter Power	-10 $[dBm]$	[27]
Receiver Sensitivity Threshold (P_{th})	-70 $[dBm]$	[27]
Noise Power (P_n)	-97 $[dBm]$	Applying the equations (2.3) and (2.4) for bandwidth $B = 28$ $[MHz]$, $T = 300$ $[K]$ and noise Figure $F =$ 2.4 $[dB]$
Minimum SINR	27 dB	$SINR_{min} = P_{th} - P_n$

4.8 Frequency Deployment Algorithms

The frequency deployment algorithm 3 presented in [1] was introduced to be the most efficient with respect to frequency reuse and network

performance. The same algorithm is used to assign frequencies when the optimized-ATPC is used.

The basic idea of the algorithm is to fade one link at a time using the maximum allowed value of fading and test if the network is still operational with respect to the SINR requirements. This operation will be repeated until all links experience the fading condition.

The above frequency deployment algorithm is modified in order to be used in optimized-ATPC. The minimum SINR criterion is replaced with a convergence checking clause. If the optimized-ATPC converges then the frequency deployment is valid and the minimum SINR constraints are met. Thus, if there are links that haven't already been faded, another link is faded and the frequency deployment is tested.

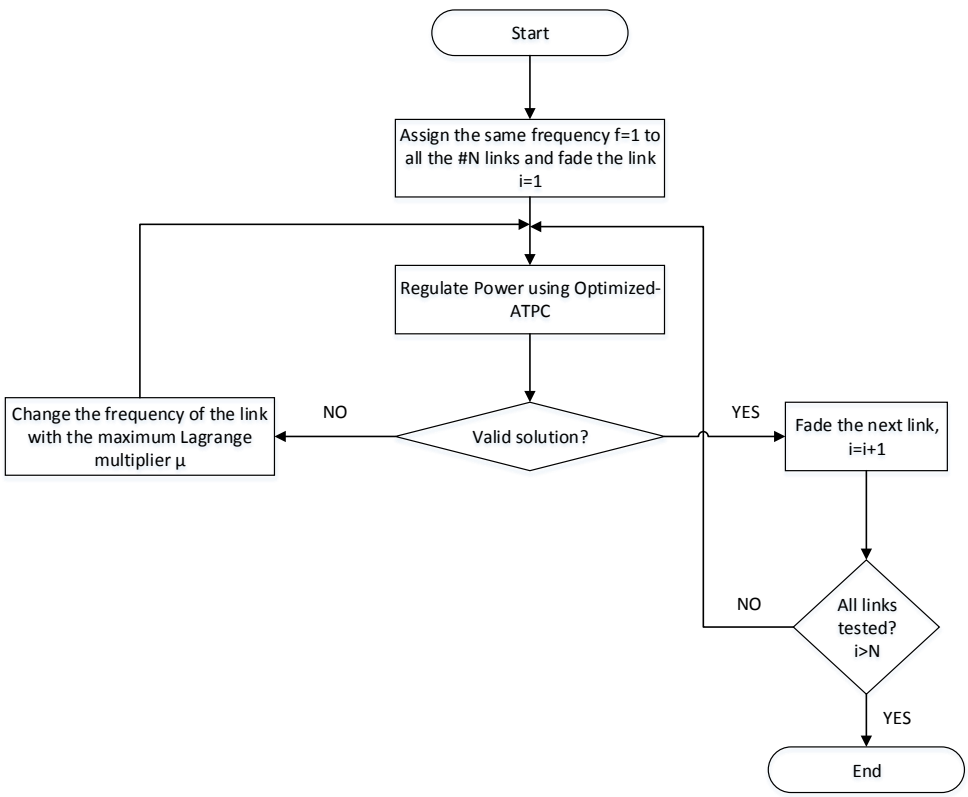

Figure 4.7: Frequency deployment algorithm

When the optimized-ATPC diverges, the frequency deployment is invalid and further frequencies must be used in MBN. The link with the highest μ multiplier value is the link with the maximum rate of increased interference (equation 3.13), and thus the link that suffers from the highest

level of interference in the network. In case of any divergence, the link which had the maximum μ multiplier before divergence will be moved to a new frequency.

One drawback of the current algorithm is that the performance can be affected by the order of links, which undergo the fading condition. The algorithm is depicted in Figure 4.7.

4.9 Performance Test

The performance of power control algorithms is compared in terms of frequency reuse and spectral efficiency. The performance test algorithm is inspecting the efficiency of the exported frequency deployment using the algorithm (Figure 4.8) during clear sky conditions and rain fading.

The goal of the performance test presented in [1] is to inspect as many propagation scenarios as possible. The exported SINR levels are utilized to compute the spectral efficiency.

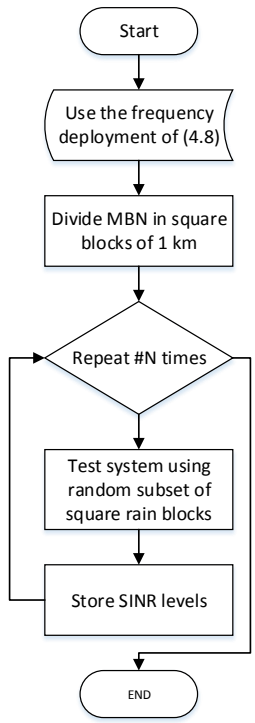

Figure 4.8: Performance test algorithm

CHAPTER 5

5 Results

In this chapter the power control algorithms hop-ATPC, node-ATPC and optimized-ATPC are compared in terms of frequency reuse and spectral efficiency. The superiority of optimized-ATPC over hop-ATPC and node-ATPC is demonstrated using different propagation scenarios and network topologies.

5.1 Introduction

For the evaluation of the power control algorithms the following network topologies (presented in section 4.5) are used:

- simple star topology
- 4-joint star topology
- real network topology

For each network topology three antennas with different radiation patterns are used:

- Fixed SLL antenna (Figure 4.4)
- Modified ETSI antenna with lower SLL (Figure 4.5)
- Modified ETSI antenna with higher SLL (Figure 4.6)

Before being able to compare the power control algorithms, the dynamic range of node-ATPC should be defined (equation 2.6). Dynamic range affects the interference level of the receivers as it determines the fixed power level that is used by the transmitters. According to the Figure 2.11, increasing the fixed margin, the node-ATPC approaches the static algorithm, while increasing the dynamic range the node-ATPC becomes fully dynamic and adaptive to the propagation conditions. As it is proved in [1], a high value of dynamic range reduces the benefits of the node cancellation technique while a high value of fixed margin reduces the gain of the dynamic power control. In order to do a fair comparison, the above trade-off was studied within this thesis. For all the network topologies and the antenna types, the spectral efficiency of the fully dynamic node-ATPC

($Dynamic\ Range = 20\ dB$) and the partially dynamic node-ATPC ($Dynamic\ Range = 10\ dB$) were simulated and compared in terms of spectral efficiency. The spectral efficiency ρ is defined as:

$$\rho = \frac{\ln(SINR)}{frequencies\ used} \tag{5.1}$$

The computed spectral efficiency is the mean spectral efficiency of the obtained SINR levels using the performance test, which is presented in chapter 4.9. The results show that the partially dynamic node-ATPC, which can benefit of the node cancellation technique, has better spectral efficiency compared to the fully dynamic node-ATPC.

In the next sections, the use of node-ATPC with dynamic range of $10\ dB$ is considered. The optimized-ATPC is compared with node-ATPC with and without cancellation.

5.2 Frequency reuse

Using antennas with different radiation patterns potentially affects the interference level in MBN. Increasing the antenna SLLs results in higher total interference level and limits the frequency reuse capability. The antenna selection is critical and the RPE significantly affects the performance of MBN. Thus, it is important to investigate the impact of RPE the number of required frequencies for different propagation scenarios to be able to perform the evaluation of the power control algorithms. The power control algorithms that can tolerate higher interference levels, when antennas with higher SLLs are used, can achieve tighter frequency reuse.

The frequency deployment algorithm in combination with the power control algorithm export a valid frequency network plan for a specific network scenario. The frequency deployment algorithm used for the node-APTC is presented in [1 - Algorithm 3] and for the optimized-ATPC in section (4.8).

The number of frequencies required by each system setup is the criterion for the frequency reuse performance; the less the required frequencies, the better the performance of the power control algorithm is.

5.2.1 Fixed SLL Antennas

In this section, the antenna type 1 with fixed SLLs, varying from -34 to $-62\ dB$, is used for the evaluation of the power control algorithms. It should be mentioned that the fixed SLL antennas do not exist in reality. By using fixed SLL antennas the impact of the different interference level to the performance of the power control algorithms as well as the impact of interference cancellation technique is shown.

The simulation results for the three different network topologies are presented in Figures 5.1 to 5.3. From the figures, it can be extracted that the optimized-ATPC outperforms the node-ATPC for high SLLs regardless of the network topology. Using fixed SLL antennas and optimized-ATPC, the frequency reuse gain reaches up to 50% compared to the node-ATPC with node cancellation and up to 75% compared to the node-ATPC without node cancellation. Furthermore, the frequency reuse gain is even higher when the optimized-ATPC is compared with hop-ATPC with and without cancellation. As far as the real network scenario is concerned, it can be found from the results that the use of interference cancellation technique does not improve the frequency reuse capability (see Figure 5.3).

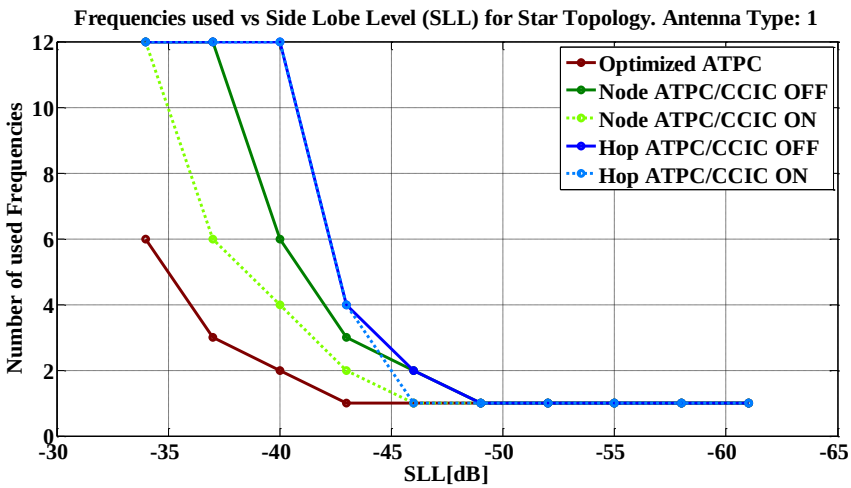

Figure 5.1: Frequency reuse comparison for the Star Topology. Antenna type 1

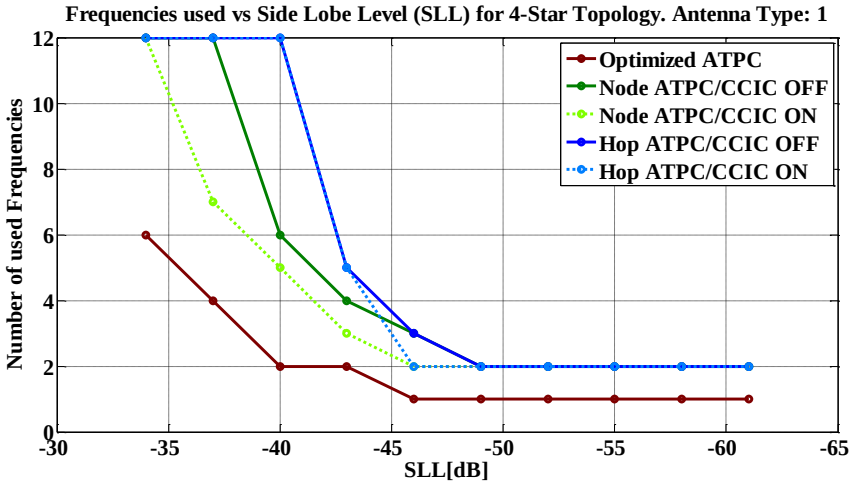

Figure 5.2: Frequency reuse comparison for the 4-Star Topology. Antenna type 1

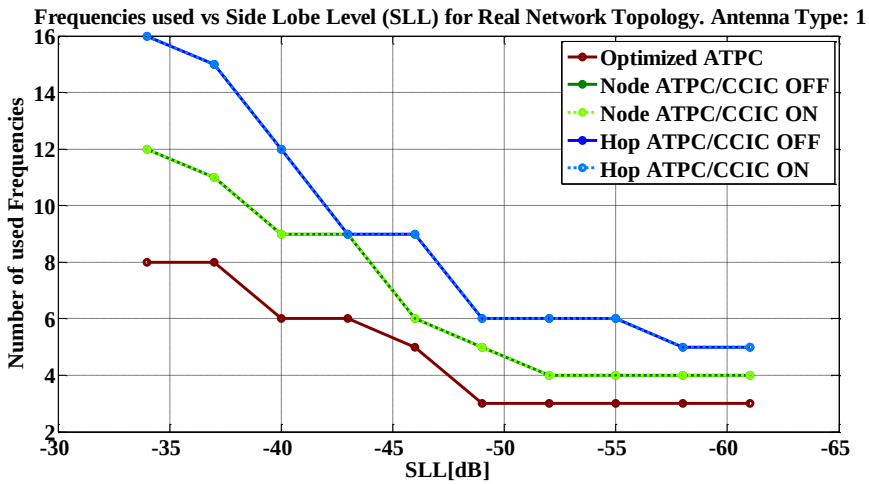

Figure 4.3: Frequency reuse comparison for the Real Network Topology. Antenna type 1

5.2.2 Modified ETSI example Antennas

In this section, the antenna types 2 and 3 with fixed SLLs, varying from -34 to $-62\,dB$, are used for the evaluation of the power control algorithms. Both antennas are modified versions of the ETSI example antenna. The basic difference between two antennas is that antenna 2 has

lower level of SLLs compared to antenna 3 and thus, antenna 2 results in lower interference level in MBN.

The simulation results for the three different network topologies are presented in Figures 5.4 to 5.9. From the figures, it can be concluded that:

- Optimized-ATPC outperforms both hop-ATPC and node-ATPC with/without node cancellation
- The number of frequencies required by the real network is the same for both node-ATPC and hop-ATPC with and without cancellation
- The antenna type has significant impact on the frequency reuse capability. The number of required frequencies decreases for antennas with lower SLLs.

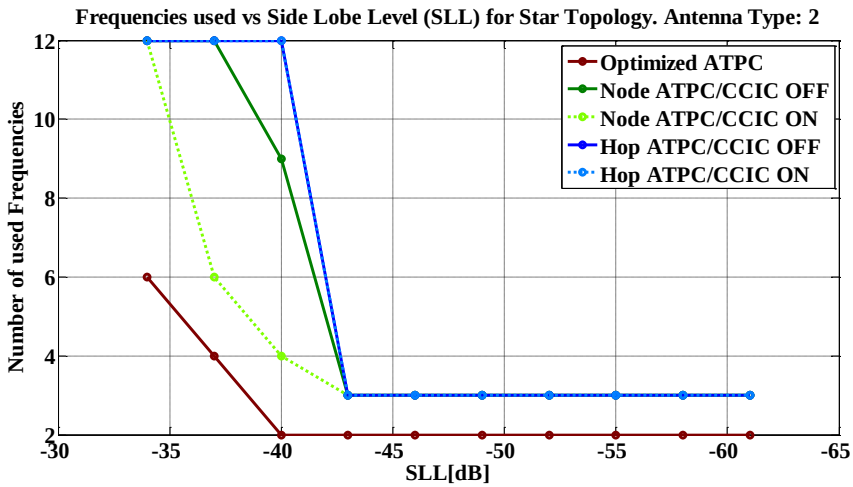

Figure 5.4: Frequency reuse comparison for the Star Topology. Antenna type 2

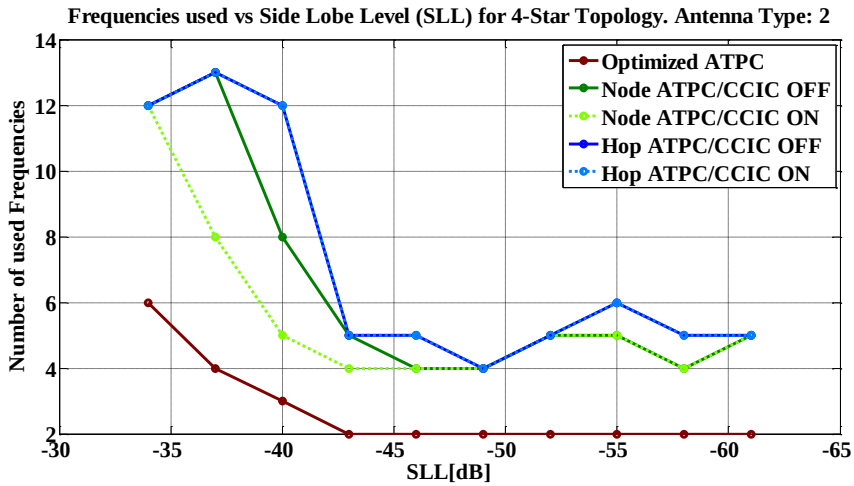

Figure 5.5: Frequency reuse comparison for the 4-Star Topology. Antenna type 2

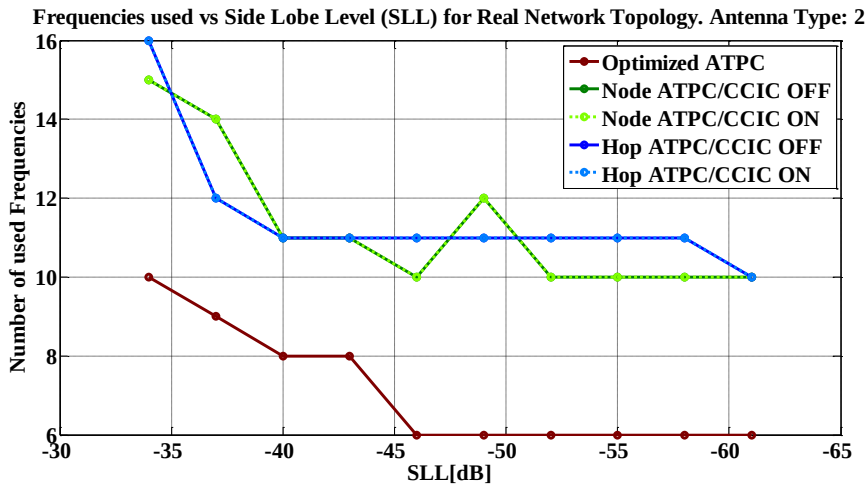

Figure 5.6: Frequency reuse comparison for the Real Network Topology. Antenna type 2

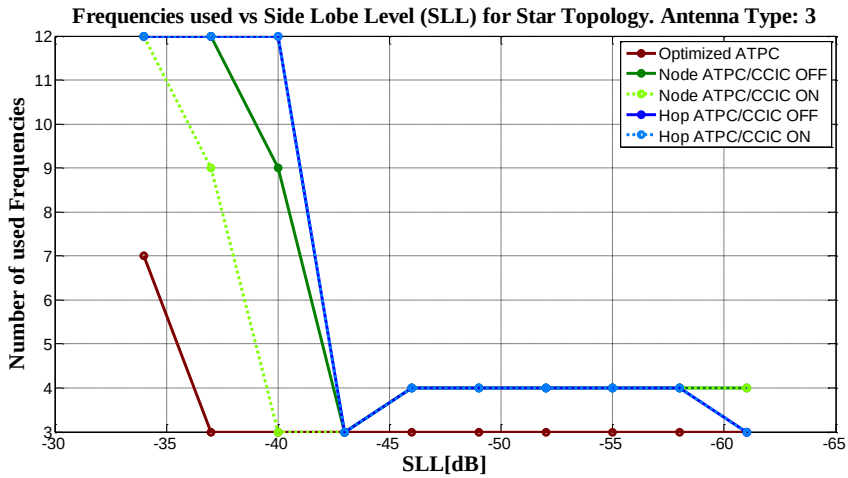

Figure 5.7: Frequency reuse comparison for the Star Topology. Antenna type 3

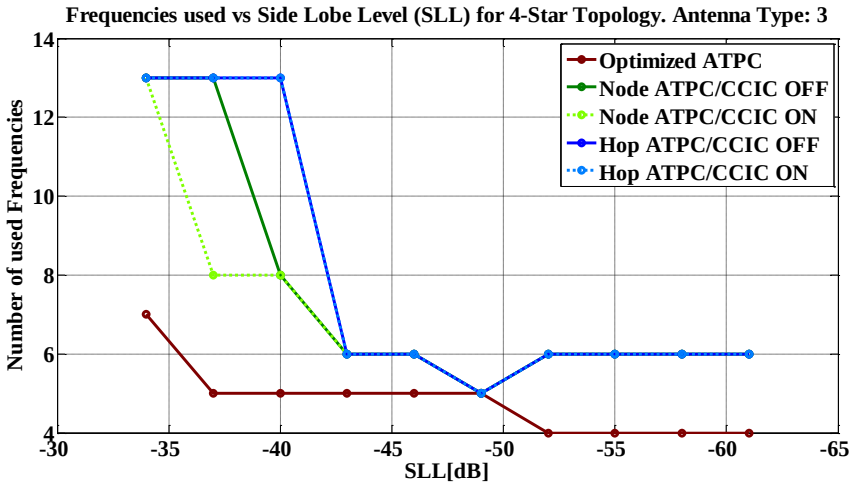

Figure 5.8: Frequency reuse comparison for the 4-Star Topology. Antenna type 3

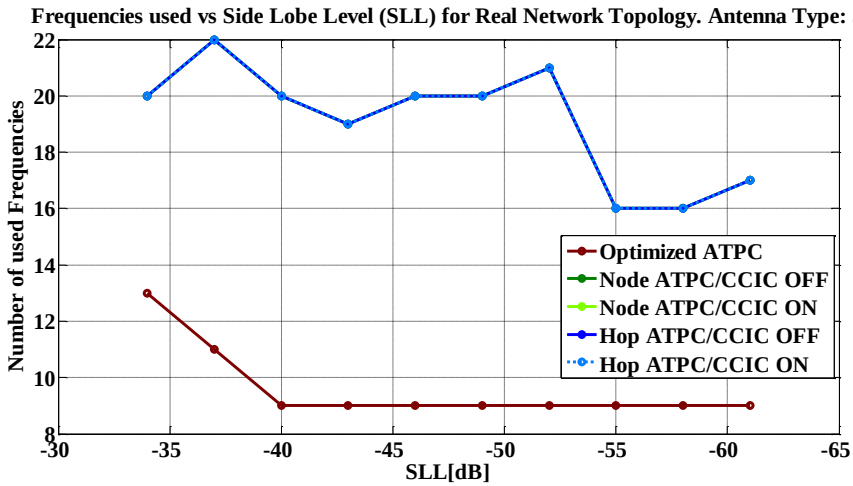

Figure 5.9: Frequency reuse comparison for the Real Network Topology. Antenna type 3

5.3 Spectral Efficiency

This section contains the spectral efficiency results obtained through the performance test described in section 4.9. The spectral efficiency is extracted by utilizing the stored SINR levels for different propagation scenarios, topologies and antenna types.

5.3.1 Fixed SLL Antennas

The spectral efficiency for the three different network topologies using fixed SLL antennas is presented in Figures 5.10 to 5.12. From the figures, it can be concluded that:

- Using a single star topology the spectral efficiency for optimized-ATPC is higher than node-ATPC and hop-ATPC except some specific SLLs.
- The difference in spectral efficiency between optimized-ATPC and both hop-ATPC and node-ATPC however becomes clearer when more complex topologies are used (4-star topology and real network topology). For these topologies, optimized-ATPC clearly outperforms node-ATPC in terms of spectral efficiency.
- The cancellation technique improves significantly the spectral efficiency when star and 4-star topologies are utilized.

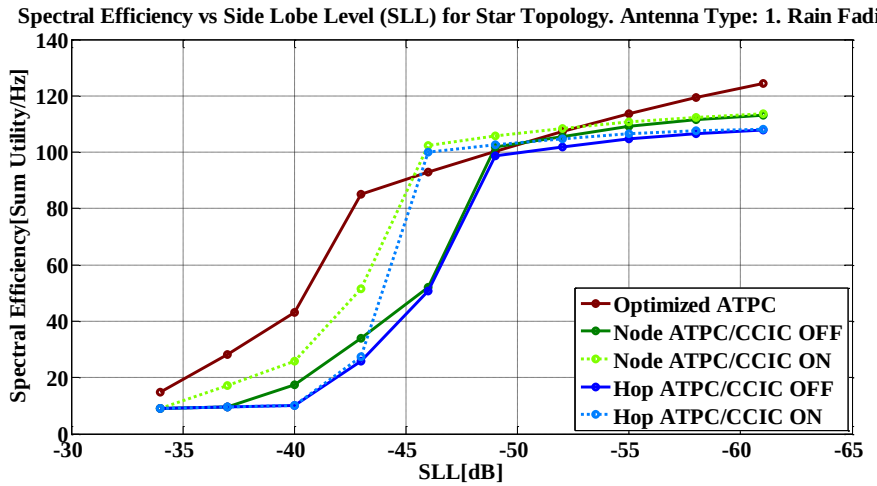

Figure 5.10: Spectral efficiency comparison for the Star Network Topology. Antenna type 1

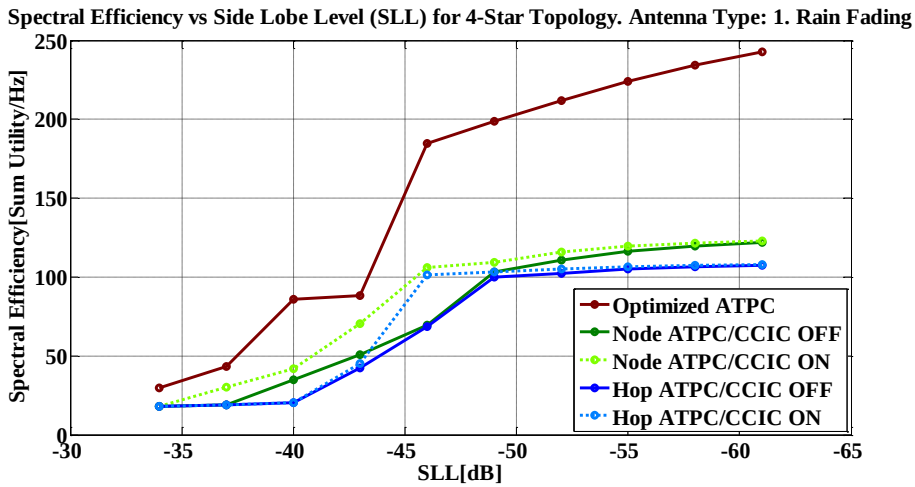

Figure 5.11: Spectral efficiency comparison for the 4-Star Network Topology. Antenna type 1

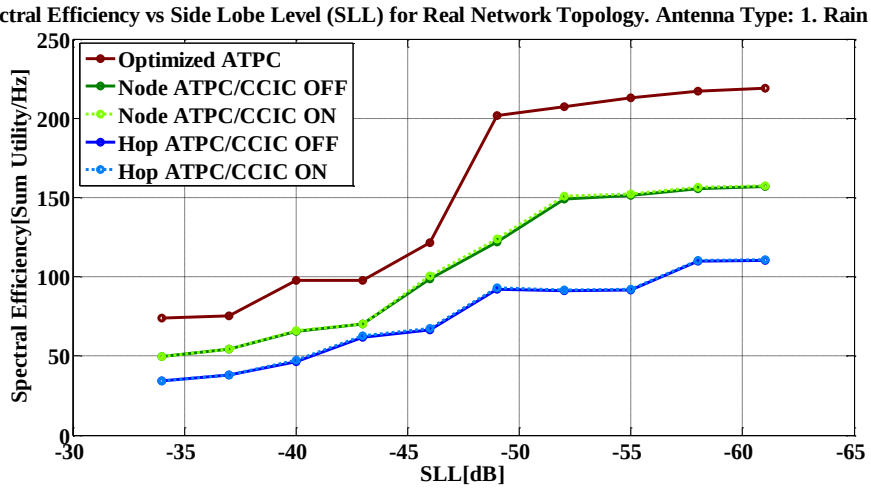

Figure 5.12: Spectral efficiency comparison for the Real Network Topology. Antenna type 1

5.3.2 Modified ETSI example Antennas

The spectral efficiency performance is depicted in figures 5.13 to 5.15, when antenna 2 is used, and in figures 5.16 to 5.18, when antenna 3 is used. When the modified ETSI example antennas are utilized, optimized-ATPC clearly outperforms both hop-ATPC and node-ATPC. Antenna type 3 results in high interference level in MBN and thus, in low SINR level and spectral efficiency. The performance difference between optimized-APTC and hop-ATPC/node-ATPC in terms of spectral efficiency is even higher in real network topology, where the node cancellation technique has minor effect.

5.4 General Observations

Considering frequency reuse in MBNs, the level of interference is increasing according to the frequency reuse factor; the tighter the frequencies reuse, the more the interference level in the MBN is.

The SINR level, which limits the frequency reuse, is minimized during fading conditions. Thus, the frequency reuse cannot be tighter during clear sky conditions. However, the spectral efficiency in the nominal case is much higher using the adaptive power control algorithms. Examining the

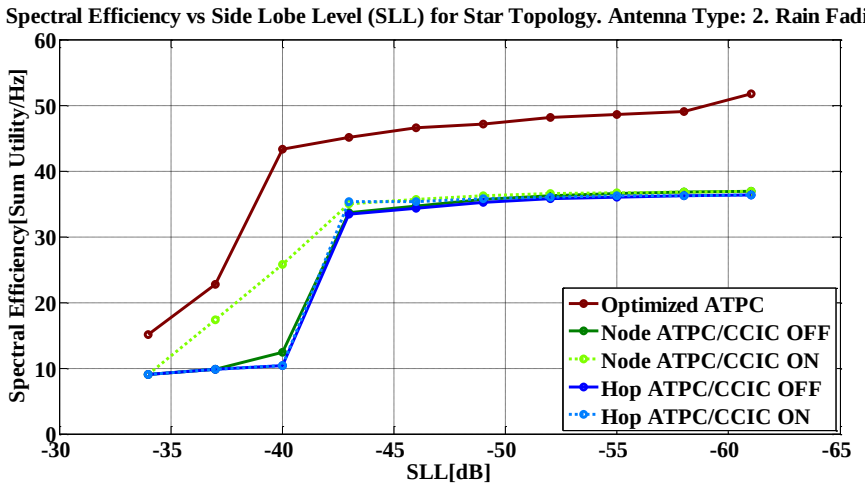

Figure 5.13: Spectral efficiency comparison for the Star Network Topology. Antenna type 2

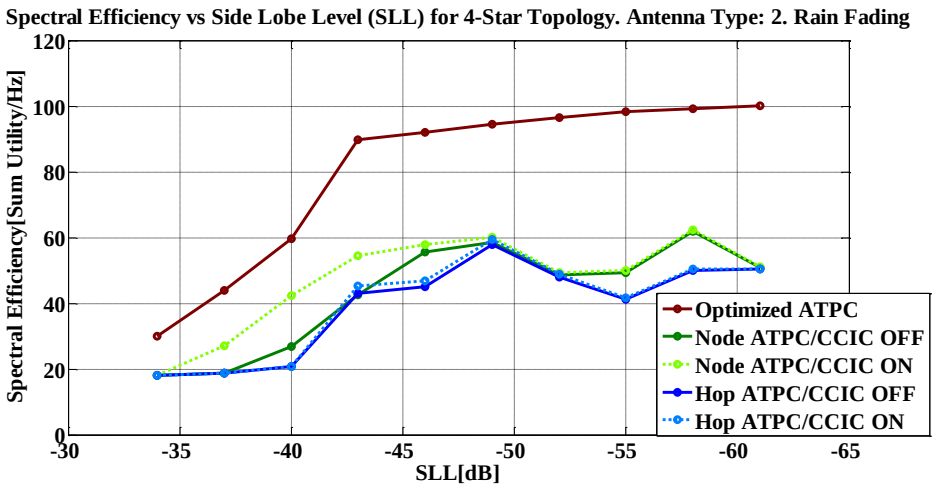

Figure 5.14: Spectral efficiency comparison for the 4-Star Network Topology. Antenna type 2

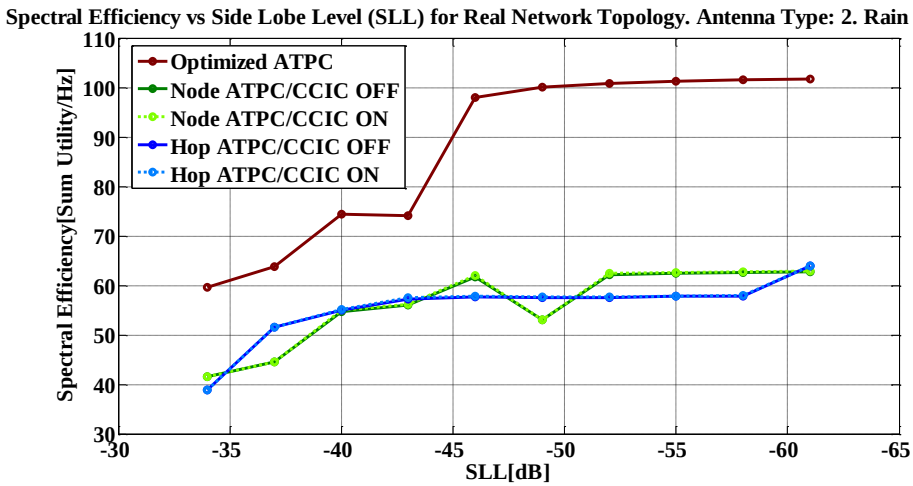

Figure 5.15: Spectral efficiency comparison for the Real Network Topology. Antenna type 2

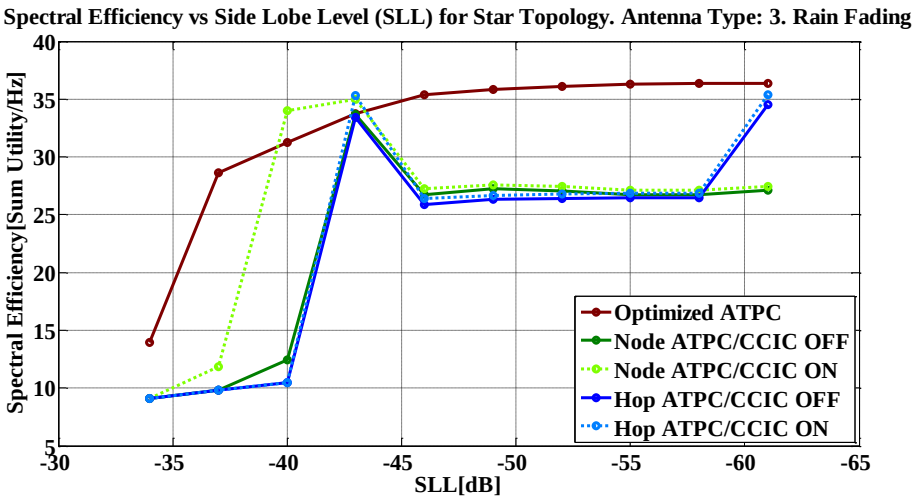

Figure 5.16: Spectral efficiency comparison for the Star Network Topology. Antenna type 3

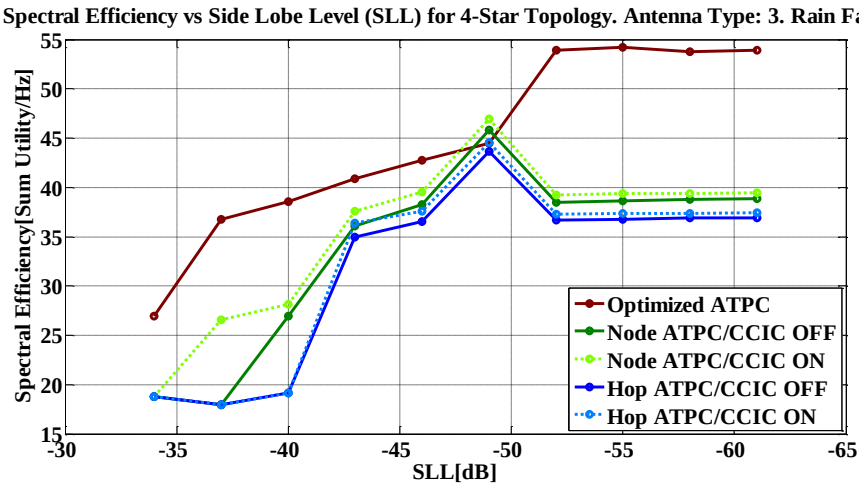

Figure 5.17: Spectral efficiency comparison for the 4-Star Network Topology. Antenna type 3

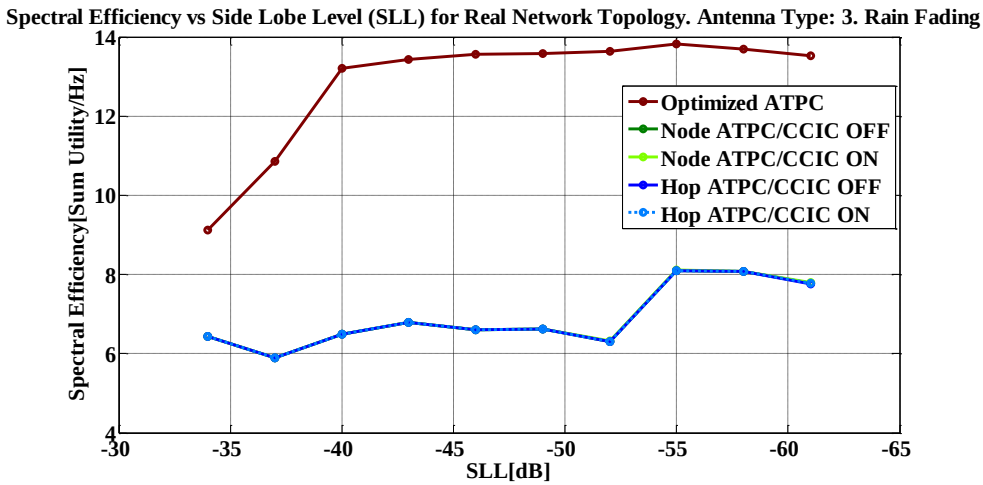

Figure 5.18: Spectral efficiency comparison for the Real Network Topology. Antenna type 3

case of the 4-star network and antenna type-3, it can be observed that the capacity of the MBN is almost doubled (Figure 5.19). This behavior is expected as the SINR levels during clear sky conditions are increased compared to the fading scenario.

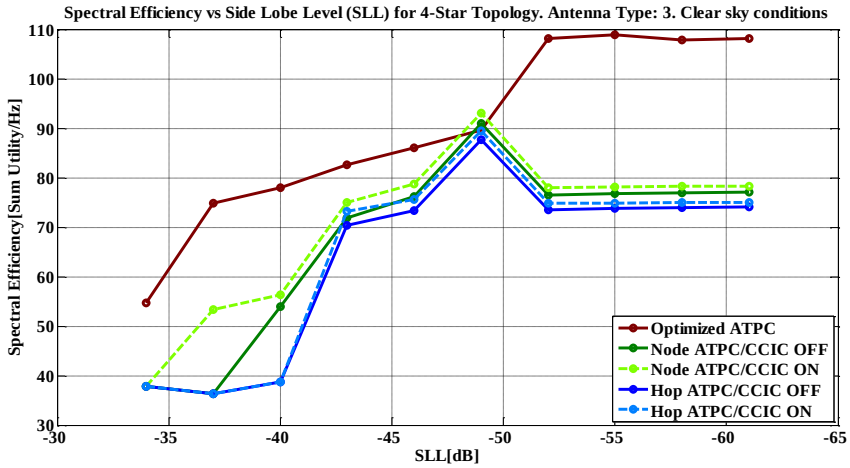

Figure 5.19: Clear sky conditions. Spectral efficiency comparison for the 4-Star Network Topology. Antenna type 3

One general observation is that the optimized-ATPC provides in significant improvement when antennas with high SLLs are used. The antennas with higher SLLs are cheaper and easy to build. Thus, a lower network cost can be achieved by utilizing cost efficient antennas in the MBN while the performance is maintained to a similar level.

After testing the frequency deployment algorithm combined with optimized-ATPC for both directions (inner to outer and outer to inner radios) and all the used network topologies, it was found that the maximum number of frequencies was used in the inner to outer communication direction. In this case, the utilization of interference cancellation does not improve the SINR level as it is impossible to apply this cancellation technique on the outer radios. Moreover, considering constant duplex communication distance, the minimum number of frequencies, which can be used for the operation of MBN, is equal to the maximum number of frequencies coming from the application of frequency deployment algorithm in both communication directions. Thus, the optimized-ATPC does not utilize any interference cancellation technique.

5.5 Assumptions and Simplifications

The power control algorithms are evaluated using a simplified model, which is described in chapter 4. This model includes many assumptions, which can affect the results.

Usually, the operators follow a manual frequency deployment process taking into consideration the link budgets, available spectrum, weather statistics, obstacles and other fading phenomena that possibly cause signal quality degradation. In the simulations, in order to easily compare the performance of the algorithms, an automatic frequency deployment process was utilized. The automatic frequency deployment process permits the evaluation of several network topologies but it does not guarantee the optimum network performance.

In addition to the star network scenario, a real network scenario is utilized for the evaluation of the power control algorithms. The star network topology corresponds to a common mobile network structure consisted by a macrocell surrounded by microcells. In this case, all the microcells are interconnected using a common node: the macrocell. The real network scenario provides an example of how the power control algorithms can be applied to existing MBNs.

A serious disadvantage of the optimized-ATPC algorithm is its computational complexity, which increases with the size of MBN. Using node-ATPC the decision for the power levels of the radios is deterministic: the power of the radios is regulated according to the power level of the others. Hop-ATPC also is a deterministic power control technique as the current propagation conditions of the links define the power levels that will be used. Furthermore, optimized-ATPC requires a global network channel matrix while node-ATPC operates in node level and hop-ATPC in hop-level.

Resuming all the results presented in chapter 5, optimized-ATPC enables tighter frequency reuse than hop-ATPC and node-ATPC. Furthermore, using optimized-ATPC is beneficial for spectrum efficiency. The capacity of the MBN is doubled in many cases.

The extracted results for the power consumption are not conclusive and further evaluation is required. In detail, it not clear which algorithm gives lower total power consumption. Depending on the topology, the antenna type and the SLL the power consumption varies. Thus, it is impossible to figure out which of the two algorithms performs better with respect to power consumption.

CHAPTER 6

6 Conclusions and Future Work

6.1 Conclusions

This thesis shows that optimized-ATPC allows tighter frequency reuse and does enable better spectrum efficiency compared to both hop-ATPC and node-ATPC with and without node cancellation. The superiority of the optimized-ATPC algorithm is noticeable in the case of real network scenario when antennas with high SLLs are used.

The automatic frequency deployment is using as criterion the minimum SINR level during rain fading. As a result, it is not possible to enable tighter frequency reuse during clear sky conditions as the SINR during rain fading is always lower.

The parameters of node-ATPC are configured during rain fading. This results in higher interference during clear sky conditions due to the fixed margin parameter. The fully dynamic optimized-ATPC algorithm does not suffer from drawback. As the transmission power level is adapted to the underlying propagation conditions. Nevertheless, this requires continuous update of the mentioned full network channel matrix.

6.2 Future Work

Examining the performance of the introduced optimized-ATPC algorithm when QoS restrictions are used could extend this thesis work. In this thesis equal QoS level is applied to all the links of the network by setting a common minimum SINR level. An operator would like to ensure better capacity or stability for some critical links of MBN. By setting a higher SINR level to these MBN links it is guaranteed that they are less sensitive to fading and a higher order modulation scheme can be supported in order to obtain higher capacity.

This thesis uses suboptimal automatic frequency deployment algorithms. The performance of the power control algorithms depends on the order that the links are faded. The operators normally apply manual frequency deployment according to the link budget calculations. However, the fully dynamic ATPC algorithms need optimized automatic frequency deployment algorithms in order to obtain the maximum MBN performance. The automatic frequency deployment algorithm optimization must be further investigated.

Optimized-ATPC technique is based on an iterative algorithm. The complexity of this algorithm is high and optimization with respect to the runtime must be considered in order to be applicable in real time. For the runtime optimization of the introduced algorithm parallelization or/and divide and conqueror techniques can be applied.

As far as the power consumption is concerned, the extracted results are not conclusive and further investigation is needed. Furthermore, more complex network topologies can be used in order to evaluate the power control algorithms.

References

[1] J. Nygårdh, “A study on frequency reuse in microwave radio link networks,” Dept. of Electrical Engineering, Linköping University (performed at Ericsson AB), Sweden, 2013.

[2] Gatsis, N.; Marques, A.G.; Giannakis, G.B., “Power control for cooperative dynamic spectrum access networks with diverse QoS constraints,” Communications, IEEE Transactions on, vol.58, no.3, pp.933,944, March 2010.

[3] Juha Salmelin and Esa Metsälä. “Mobile Backhaul”. WILEY. Cited on Chapter 1.

[4] Ericsson Annual Report 2010, Stockholm, Sweden, March 2011. http://www.ericsson.com/thecompany/investors/financial_reports/2010/annual10/sites/default/files/Ericsson_AR_2010_EN.pdf.

[5] Ericsson Annual Report 2012, , Stockholm, Sweden, November 2013. http://www.ericsson.com/res/investors/docs/2012/ericsson-ar-2012-en.pdf

[6] Jonas Hansryd and Jonas Edstam. “Microwave Capacity Evolution”. In Ericsson Review, Vol 1, 2011. http://www.ericsson.com/res/docs/review/Microwave-Capacity-Evolution.pdf.

[7] Callaghan, S.A.; Inglis, I.; Hansell, P., “Spectrum efficiency gains resulting from the implementation of adaptive transmit power control in fixed terrestrial links at 38 GHz,” Antennas and Propagation, 2006. EuCAP 2006. First European Conference on, vol., no., pp.1, 6, 6-10 Nov. 2006

[8] XPIC Function in PT http://erilink.ericsson.se/eridoc/erl.html?objectId=09004cff8753f688&action=approved&format=msw8&DocNo=2%2F102+62-CRH+109+0906%2F1+Uen

[9] Ericsson AB, “High-speed mobile backhaul demonstrators”. White Paper, 2009.

[10] Trojer, E., Dahlfort, S., Hood, D. and Mickelsson, H.: Current and next-generation PONs: A technical overview of present and future PON technology. Ericsson Review, Vol. 85(2008)2, pp. 64–69

[11] Harvey Lehpamer. "Microwave Transmission Networks". The McGraw-Hill Companies, 2nd edition.

[12] Martin P. Clark. "Wireless Access Networks". JohnWiley & Sons LTD.

[13] Simon R. Saunders and Alejandro Aragón-Zavala. "Antennas and Propagation for Wireless Communication Systems". WILEY, 2nd edition.

[14] P. Hansell. S.A. Callaghan, I. Inglis. "Impact of introducing Automatic Transmit Power Control in P-P Fixed Service systems operating in bands above 13 GHz". Technical report, Ofcom, February 2006.

[15] Dan Weinholt. "Power Control of a Radio System". Patent Cooperation Treaty WO 2011/079858 A1, 2011.

[16] Saad Z. Asif. "Next Generation Mobile Communications Ecosystem – Technology Management for Mobile Communication". WILEY, first edition edition.

[17] European Standard (Telecommunications series). Fixed Radio Systems ETSI EN 302 217-4-2, 2008-11 edition.

[18] Recommendation ITU-R P.526-12. "Propagation by diffraction", 2012.

[19] C. E. Shannon (January 1949). "Communication in the presence of noise"

[20] Jianwei Huang; Berry, R.A.; Honig, M.L., "Distributed interference compensation for wireless networks," Selected Areas in Communications, IEEE Journal on , vol.24, no.5, pp.1074,1084, May 2006 doi: 10.1109/JSAC.2006.872889

[21] Stanczak, S.; Wiczanowski, M.; Boche, H., "Distributed Utility-Based Power Control: Objectives and Algorithms," Signal Processing, IEEE Transactions on , vol.55, no.10, pp.5058,5068, Oct. 2007 doi: 10.1109/TSP.2007.897856

[22] M. Wiczanowski, “Algorithmic and analytic framework for optimization of multi-user performance in wireless networks with interference,” Ph.D. dissertation, Dept. Elect. Eng. Comput. Sci., Tech. Univ. Berlin, Berlin, Germany, 2007.

[23] S. Stanczak, M. Wiczanowski, and H. Boche, Resource Allocation in Wireless Networks: Theory and Algorithms. Berlin, Germany: Springer, 2006.

[24] Boche, H.; Stanczak, S., “Convexity of some feasible QoS regions and asymptotic behavior of the minimum total power in CDMA systems,” Communications, IEEE Transactions on , vol.52, no.12, pp.2190,2197, Dec. 2004

[25] Boyd and Vandenberghe, “Convex Optimization”, Cambridge University Press

[26] Recommendation ITU-R P.838-2. "Specific attenuation model for rain for use in prediction methods", 2003.

[27] Ericsson AB. "MINI-LINK TN". Product Sheet. http://prodcat.ericsson.se/frontend/category.action?code=FGB%20101%20004&path=\Navigation%20Root\FGA%20101%2017

List of Acronyms

MBN	Microwave Backhaul Network
ATPC	Automatic Transmitter Power Control
SINR	Signal-to-Interference-plus-Noise Ratio
FDD	Frequency Division Duplex
BER	Bit Error Rate
XPIC	Cross-Polarization Interference Cancellation
RBS	Radio Base Station
LRAN	Low Radio Access Network
HRAN	High Radio Access Network
HSPA	High Speed Packet Access
LTE	Long Term Evolution
OFDM	Orthogonal Frequency Division Multiplexing
MIMO	Multiple-Input and Multiple-Output
ITU	International Communication Union
ITU-R	ITU Radiocommunications Sector
CEPT	Conference of European Post and Telecommunications
FCC	Federal Communications Commissions
SNR	Signal-to-Noise-Ratio
PLL	Phase Locked Loop
CIR	Carrier to Interference Ratio
BS	Base Station
BSC	Base Station Controller
MTBF	Mean Time between failure
QAM	Quadrature Amplitude Modulation
BPSK	Binary Phase Shift Keying
CCDP	Co-Channel Dual Polarized
RPE	Radiation Pattern Envelope
FSPL	Free-space path loss
XPD	Cross-Polar Discrimination
SLL	Side Lobe Level

Appendix 1

A.1 Calculation of Diffraction Loss

Parameter v is defined as the parameter for the path clearance and it calculated using the following formulas (Figure):

$$d = d_1 + d_2 \qquad (A.1)$$

$$v = \sqrt{\frac{2d}{\lambda} tan\alpha\ tan\beta} = \sqrt{\frac{2d}{\lambda}\frac{h}{d_1}\frac{h}{d_2}} = h\sqrt{\frac{2(d_1 + d_2)}{\lambda d_1 d_2}} \qquad (A.2)$$

The parameter v is positive for obstructed paths and negative for clear LOS paths. Based on the theory of the diffraction of electric fields over a knife edge and the value of the parameter v, the loss may be approximated by:

$$A(v) \approx \begin{Bmatrix} 6.02 + 9v + 1.65v^2, & -0.8 \le v \le 0 \\ 6.02 + 9.11v - 1.27v^2, & 0 < v \le 2.4 \\ 12.953 + 20logv, & v > 2.4 \end{Bmatrix} \qquad (A.3)$$

A.2 Descent methods

A.2.1 General Description

The descent methods [25] are used to produce a minimizing sequence $x^{(k)}, k = 1, ...$, where:

$$x^{(k+1)} = x^{(k)} + t^{(k)}\Delta x^{(k)} \qquad (A.4)$$

The term $\Delta x^{(k)}$ is called *search direction* and the scalar $t^{(k)} \ge 0$ is called *step length* at iteration k. The method that is used for the solution search of (3.9) is descent, which means that:

$$f\left(x^{(k+1)}\right) < f\left(x^{(k)}\right) \qquad (A.5)$$

except when $x^{(k)}$ is optimal From (3.11) it can be implied that all $x^{(k)}$ must belong to the domain of the function, $x^{(k)} \in \boldsymbol{dom} f$. This property can be used for the initialization step of the descent method algorithms, as the initialization vector $x^{(0)}$ should belong to the domain of the function.

The general descent method is depicted in Figure A.1. A descent direction Δx is determined and a step size t is selected. The line search of the step size t determines where along the line $\{x + t\Delta x | t \epsilon \mathbb{R}_+\}$ the next search will be. The stopping criterion is often of the form $\|\nabla f(x)\|_2 \leq \eta$, where η is small and positive.

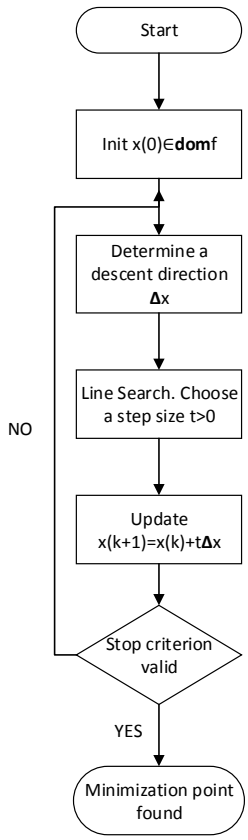

Figure A.1: General Descent Method

A.2.2 Gradient Descent Method

When the negative gradient $\Delta x = -\nabla f(x)$ is selected for the search direction, the resulting algorithm is called gradient algorithm or gradient descent method [25]. The algorithm that will be used for the minimization of the equation (3.9) is using constant step distance $t = \beta$. The algorithm is illustrated in Figure 3.2.

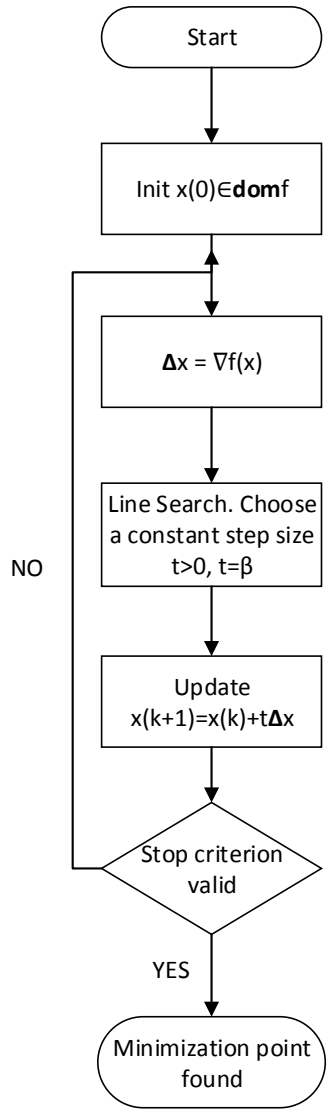

Figure 3.2: Gradient descent method

LUND
UNIVERSITY

http://www.eit.lth.se